

Shaping Magnetic Fields to Direct Therapy to Ears and Eyes

B. Shapiro,^{1,2} S. Kulkarni,¹ A. Nacev,¹ A. Sarwar,¹
D. Preciado,³ and D.A. Depireux²

¹Fischell Department of Bioengineering, ²The Institute for Systems Research (ISR), University of Maryland, College Park, Maryland 20742; email: benschap@umd.edu

³Otolaryngology, Sheikh Zayed Institute for Pediatric Surgical Innovation, Children's National Medical Center, Washington, DC 20010

Annu. Rev. Biomed. Eng. 2014. 16:455–81

The *Annual Review of Biomedical Engineering* is online at bioeng.annualreviews.org

This article's doi:
10.1146/annurev-bioeng-071813-105206

Copyright © 2014 by Annual Reviews.
All rights reserved

Keywords

magnetic targeting, drug delivery, ear, eye, nanotherapy, stem cells

Abstract

Magnetic fields have the potential to noninvasively direct and focus therapy to disease targets. External magnets can apply forces on drug-coated magnetic nanoparticles, or on living cells that contain particles, and can be used to manipulate them in vivo. Significant progress has been made in developing and testing safe and therapeutic magnetic constructs that can be manipulated by magnetic fields. However, we do not yet have the magnet systems that can then direct those constructs to the right places, in vivo, over human patient distances. We do not yet know where to put the external magnets, how to shape them, or when to turn them on and off to direct particles or magnetized cells—in blood, through tissue, and across barriers—to disease locations. In this article, we consider ear and eye disease targets. Ear and eye targets are too deep and complex to be targeted by a single external magnet, but they are shallow enough that a combination of magnets may be able to direct therapy to them. We focus on how magnetic fields should be shaped (in space and time) to direct magnetic constructs to ear and eye targets.

Contents

1. INTRODUCTION	456
2. DRUG DELIVERY TO THE INNER EAR	457
3. DRUG DELIVERY TO THE MIDDLE EAR	463
4. THERAPY DELIVERY TO THE EYE	463
5. NEEDS AND FUTURE DIRECTIONS	468

1. INTRODUCTION

A large fraction of the drugs we administer to patients does not go where we want it to go. During systemic chemotherapy, animal experiments indicate that less than 0.1% of the drugs is taken up by tumor cells, with the remaining >99.9% going into healthy tissue (1). In topical delivery to the eye, only approximately 1–10% of the applied small drug molecules permeate the eye (2). For the inner ear, just 1 out of every 10^7 drug molecules administered systemically reaches the cochlea (3), in part because the cochlea, like the brain, is behind a blood–labyrinth barrier (4, 5). Having only a small fraction of therapy reach the physical location where disease occurs decreases therapeutic effect and increases side effects. Thus there is a clear and broad need to better direct and focus therapy to disease locations, for multiple clinical indications.

In magnetic targeting, therapeutics are typically attached to magnetic nanoparticles, and this enables applied magnetic fields to manipulate the therapy inside the body (6–9). The type of therapies that can be associated with magnetic materials is diverse. To date, chemotherapy and hyperthermia directed by magnetic nanoparticles have been tested in human Phase I/II trials (7, 10–13). Specifically, using chemotherapy bound reversibly to the polymer coatings of the particles, Lübbecke et al. (7) reported the resulting pharmacokinetics with and without an applied magnet. Magnetic thermotherapy, in which nanoparticles are heated by an applied alternating magnetic field, has been combined with radiotherapy to treat patients with recurrent glioblastomas (14). Magnetically guided gene therapy has been demonstrated in animal trials (15, 16), as well as magnetic manipulation of micelles, liposomes, and microbubbles loaded with magnetic materials (17–19). Magnetic nanoparticles have also been targeted across the intact blood–brain barrier (20). They have been used to block tumor blood vessels in a chicken embryo (21) and to trigger cellular events in cell cultures (22, 23). Live cells, such as human mesenchymal stem cells, have been cultured in media containing magnetic nanoparticles, have endocytosed the particles, and have then been magnetically directed to targets in animal experiments (24–34). Thus there is a wide range of therapies that can be manipulated magnetically.

Compared with light, electric fields, and ultrasound for manipulating therapy (35–39), magnetic fields have the advantage that they can safely penetrate deep into the body and could, in principle, direct magnetized therapy to deep tissue targets. Strong magnetic fields are routinely applied to patients during magnetic resonance imaging (MRI) (40–43), and human and animal magnetic drug targeting studies have employed magnetic fields of equal or lesser strength (7, 44, 10, 45–50, 20, 51–60). Magnetic carriers are being coupled with antibody and nucleotide targeting (61–64) to combine the long-range manipulation that magnetic fields enable with the precision molecular recognition of receptor–ligand binding.

Eighteen years after the first human clinical trials with magnetic nanoparticles (7), there is now a body of evidence that indicates magnetic materials can be used *in vivo* and that safe magnetic fields (e.g., at or below MRI strength) can manipulate them inside the body. Yet being able to apply a magnetic force to move nanoparticles *in vivo* is not the same as directing them—through tissue

barriers or against blood flow—to specific disease locations in humans. The majority of *in vivo* magnetic drug targeting demonstrations have been carried out in small animals. However, applied magnetic forces decay rapidly with distance away from magnets (65–67); thus it is more difficult to create sufficient forces on nanoparticles for the larger magnet-to-particle distances required for human patients. Further, being able to apply a sufficiently strong force is not enough. The motion of nanoparticles *in vivo* is complicated: They can be distributed by blood flow and taken up by macrophages, and their motion can be reduced, constricted, or prevented by anatomical barriers (membranes, blood vessel walls). Applied magnetic fields need to be chosen smartly to direct magnetized therapy to disease targets. To the degree possible, based on available knowledge, magnetic fields should be designed (shaped) to direct therapeutics to clinically relevant targets, across human (not small-animal) distances, using acceptable magnetic field strengths and practical magnet designs.

In this article, we focus on emerging efforts to enable magnetic drug targeting to ear and eye targets in human patients. The necessary manipulation distances are on the order of 2 to 5 cm, and the magnetic field strengths required can be achieved by current and emerging magnet systems. At the end of the article, we briefly identify needs and challenges to enable deeper targeting, such as to deep-seated tumors.

The majority of magnetic targeting research to date has focused on fabricating magnetic particles or other types of magnetic carriers [rods, shells, cubes, dumbbells, nanowires, hollow cubes, hollow spheres, discs, triangles, and tetrapods (68–84)], on linking therapeutics to these carriers (with a view toward a variety of clinical needs), and on testing the safety and efficacy of such constructs. These are critical and ongoing efforts, and they are surveyed in a number of high-quality review articles (13, 85–90). However, this is not enough—it implicitly assumes that once safe, therapeutic magnetic constructs are achieved, then there will be magnet systems available to effectively direct them to the desired clinical targets. In fact, such magnetic systems do not yet exist. Our goal in this article is to focus on the progress and challenges in constructing permanent and electromagnet systems that will direct therapy to where it needs to go, in human patients, for eye and ear diseases.

2. DRUG DELIVERY TO THE INNER EAR

There are a variety of diseases associated with the inner ear—for example, sudden sensorineural hearing loss (SSNHL), tinnitus (a ringing or roaring in the ears), and Ménière's diseases (91), which respectively affect 5,000–20,000 (92), 15 million (93), and 600,000 (94) people per year in the United States. Although it is thought that existing drugs can be effective (e.g., steroids to suppress inner ear inflammation that is thought to lead to SSNHL and tinnitus), these drugs do not effectively reach the inner ear (95, 96) because it is isolated by a blood–labyrinth barrier (97) (similar to the blood–brain barrier). Vessels that bring blood to the inner ear have walls that are largely impermeable even to small drug molecules (5). Thus drugs that are taken orally or are systemically administered into the bloodstream either do not elute or elute only poorly into inner ear tissues (98).

High-dose oral and intravenous steroid administration have been attempted as clinical therapies for sudden sensorineural hearing loss (SSNHL), with varying outcomes (99–103). Such high doses of orally or systemically administered steroids are known to cause substantial side effects (104–106). Moreover, orally or systemically administering steroids also leads to variable dosing of the inner ear space (5, 107).

Currently, there are no minimally invasive topical delivery methods for the inner ear. Although it is possible to access the middle ear by a syringe inserted through the ear canal (see

transtympanic injection discussed next), it requires an invasive mastoidectomy facial-recess surgery under general anesthesia to inject drugs into the cochlea (108, 109). To instead deliver therapy to the inner ear via the ear canal would require delivering the therapy first through the tympanic membrane and then through either the round window membrane (RWM) or the oval window membrane (OWM) (see **Figure 1a**). However, there is no line of sight from the ear canal to the

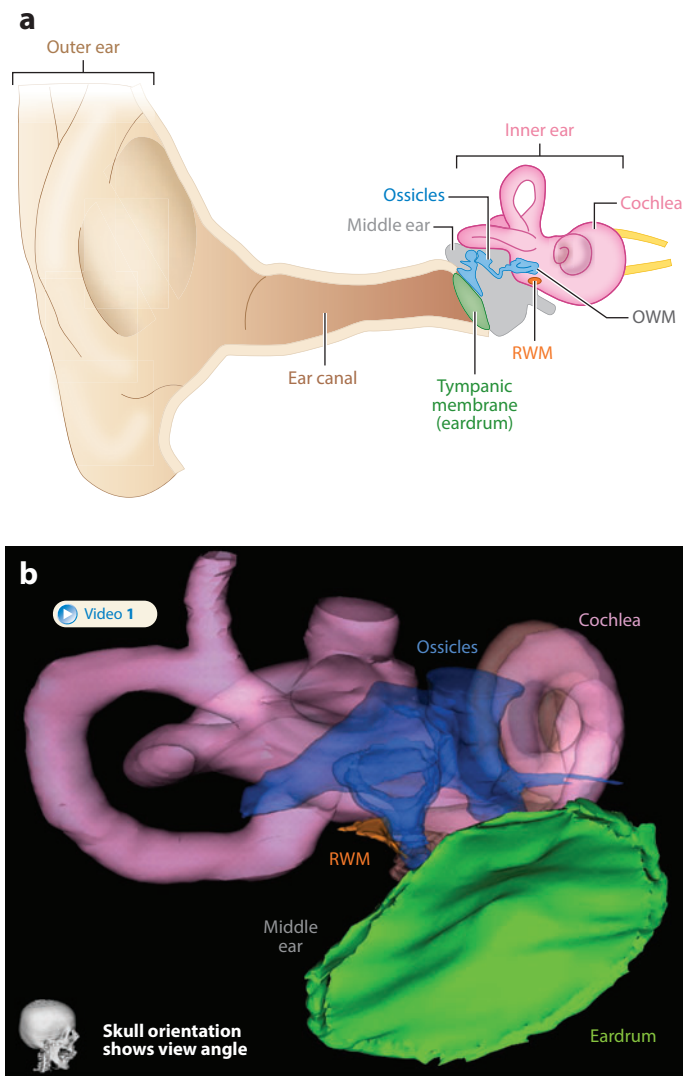


Figure 1

The human ear anatomy. (a) Schematic of the outer (*brown*), middle (*grey*), and inner ear (*pink*). The tympanic membrane (eardrum) separates the outer from the middle ear, and the oval (OWM) and round window membranes (RWM) separate the inner from the middle ear. (b) Three-dimensional visualization of the human ear anatomy achieved by surface rendering of archival sections of the temporal bone of a 14-year-old male (110). The tympanic membrane (eardrum) is shown in green, the ossicles are shown in transparent blue, the inner ear is marked in pink with the cochlea spiral at the top right, and the RWM is visible in orange side-on, diagonally above the middle ear space. **Video 1** shows the ear anatomy rotating. (Panel adapted from 111 with permission from Massachusetts Eye and Ear Infirmary © 2013.)

Clinical Trade-Off Between Control of Drug Level and Risk

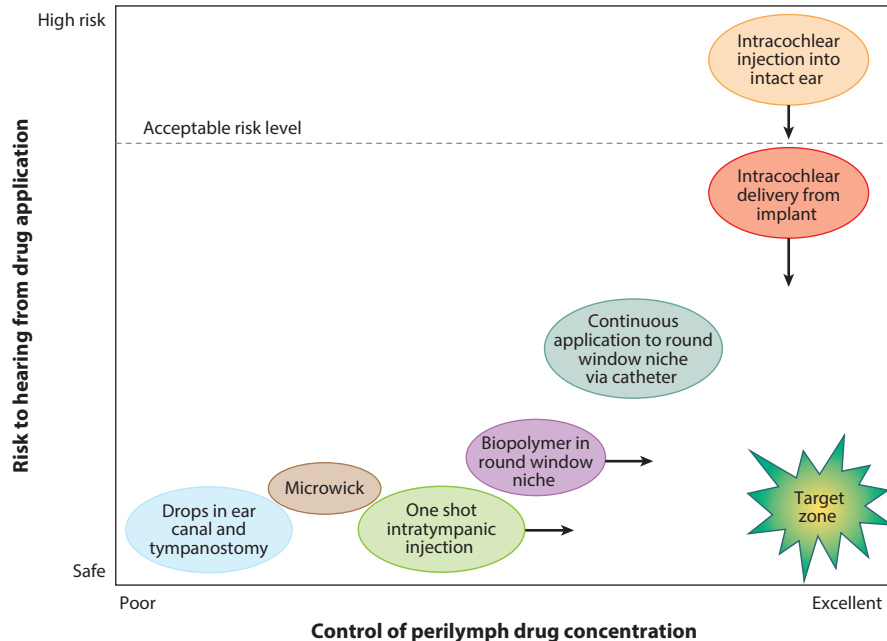


Figure 2

The current state of the art in reaching the inner ear (the perilymph is the fluid inside the two outer compartments of the cochlea). Available treatment procedures are graphed against desirable drug concentration (from poor to excellent) and the risk of the procedure (from safe to high risk). [Figure reproduced with permission from Salt & Plontke (114); ©2009 S. Karger AG, Basel.]

RWM and OWM, and most of the OWM is covered by a small bone (the third ossicle). Surgically accessing and puncturing these delicate window membranes carries risks of acoustic and vestibular trauma.

The current standard of care for SSNHL is to inject a large dose of drugs into the middle ear and wait for passive diffusion into the inner ear (102, 112). Transtympanic (through the eardrum) injection of drugs into the middle ear can be done using a syringe, through a tube (a tympanostomy), or via a microcatheter, and the eardrum heals after these procedures (91). However, subsequent diffusion of the drug from the middle ear through the window membranes and into the inner ear is limited (96, 113) and results in a steep drug concentration gradient inside the cochlea leading to too-high concentrations at the base of the cochlea with too-low concentrations in the remainder of the cochlea (114). The success of transtympanic administration of steroids to treat SSNHL has ranged from 0% to 100%, depending on various factors such as time from onset of hearing loss to treatment, extent of hearing loss, and the criteria for successful recovery (101, 102, 115). Despite the lack of consistent positive outcomes for transtympanic drug administration, it is a routine strategy for treating inner ear diseases (116).

Thus, overall, there is currently no inner ear drug delivery method that is minimally invasive, safe, and effective, as shown schematically by **Figure 2** (adapted from 114). However, there is a consensus that increasing the drug dose delivered into the inner ear could improve therapeutic effect (3, 95, 102, 114, 117–119). Strategies for prolonging the exposure of the RWM to middle-ear high steroid concentrations, so as to increase drug delivery to the inner ear, include

the placement of microcatheters, gels, and nanoparticle formulations. The Silverstein MicroWick was used for SSNHL treatment and employed a 1-mm \times 9-mm polyvinyl acetate wick that was applied through a tube in the tympanic membrane to overlie the RWM (116); it was removed from the market owing to technical administration difficulties and the potential for long-term hearing loss (120, 121). Delivery of medications to the inner ear using a microcatheter placed on the RWM was used for treatment of tinnitus associated with Ménière's disease (122). However, this method suffered from catheter dislocations and obstructions, granuloma formation within the middle ear, and permanent tympanic membrane perforations (123). Catheter dislocations resulted from the partly implantable aspect of the catheter, which was later improved by using an adhesive over the external portion of the device (116). A hydrogel system has also been used to deliver medication to the inner ear (116, 118). It offers advantages as a delivery vehicle because it is a dissolvable matrix that can be combined with the drug (116, 124–126). Potential disadvantages include the need for accuracy in placing the hydrogel in the round window (RW) niche, in contact with the RWM, and the danger of overfilling the middle ear with the hydrogel (which can lead to loss of hearing) (116).

In 2008, Kopke and coworkers (127) showed that magnetic forces could be used to effectively direct materials into the inner ear. In guinea pigs and rats, they surgically exposed the middle ear and placed superparamagnetic iron oxide nanoparticles (SNPs) into the RW niche. The animals were then placed so that the RWM of the tested ear was oriented horizontally facing upward and positioned above the center surface of a 4-inch cube, \sim 0.41-T neodymium iron boron (NdFeB-48) magnet. The distance from the RWM to the magnet was 2.5 cm for the rats and 3 cm for the guinea pigs. The authors found that the magnetic forces actively transported nanoparticles across the RWM, from the middle into the inner ear.

Kopke's approach circumvented the blood–cochlea barrier with nanotherapeutic particles and magnetic fields—it showed that instead of delivery via the blood stream, drug-coated particles could be placed into the middle ear, and then magnetic forces could be used to pull the particles (and thus drugs) into the inner ear. However, using a magnet to pull the particles into the inner ear does not scale up to humans effectively. For an adult person, a magnet pulling through the width of the human head would need to be positioned 12–15 cm away from particles placed into the contralateral middle ear. Because forces applied on the particles fall off quickly with the distance from a magnet (65, 66), the required pull magnet would need to be extremely strong. A calculation similar to the one carried out for **Figure 4b** below shows that applying the same forces across the RWM as in Kopke, but pulling across a \geq 12-cm human RWM-to-face distance, would require a \geq 13-T magnet. This number substantially surpasses the magnetic field strengths used in MRI (40) and also exceeds published safety limits (128).

Ferromagnetic nanoparticles basically act like iron filings—that is, any single magnet will always attract (pull in) the particles, regardless of the orientation of the magnet (see **Figure 3** and Sidebar, Physics of Magnetic Fields and Particles). That is why Kopke used a pull configuration in his animal experiments. If it were possible to magnetically inject (push away) particles, that would permit a magnetic device to be used at a much shorter 3–4-cm working distance for adult patients (the average face-to-cochlea distance in humans) and could allow reasonable magnets to apply sufficient forces to direct therapy into the inner ear.

It turns out that it is possible to configure magnets in such a way that the magnetic field is shaped to push nanoparticles away (137). Because magnetic particles experience a force from low to high applied magnetic field intensity, the key idea is to arrange the magnetic field intensity so that it increases away from the magnetic device in a desired (push) region. This can be done by creating a magnetic field cancellation behind the particles. The magnetic field intensity will increase going outward from that cancellation node, and so forces will point away from the device

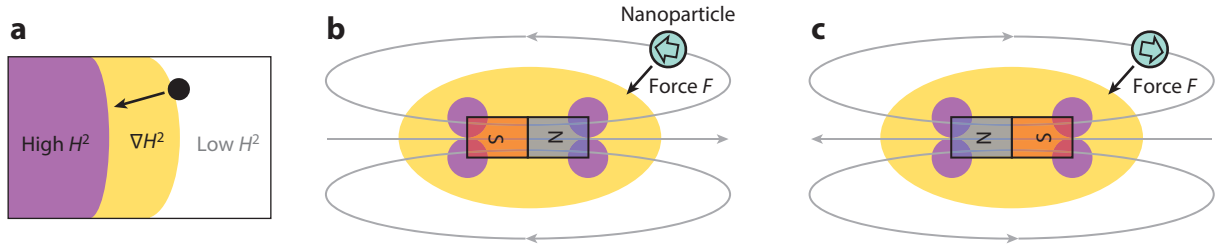


Figure 3

Ferromagnetic particles are attracted to regions of highest magnetic field intensity (the magnet corners). (a) A ferromagnetic particle (black dot) experiences a magnetic force F (arrow) from low to high (white to purple) magnetic field intensity squared (H^2). Thus (b) a single permanent magnet attracts particles to its corners where the magnetic field intensity is highest, and (c) this force remains unchanged if the polarity of the magnet is reversed (gray curves show the magnetic field lines; the open arrow shows the corresponding magnetization direction inside the particle). (©2012 IEEE; figure reprinted with permission from 88.)

on the other side of the node, as shown by the orange dot and force arrow in **Figure 4a**. The design, optimization, and construction of such a push system are described elsewhere (136–138). **Figure 4b** shows the advantage of push versus pull for human patients. For push (green) and pull (blue) systems of comparable size and strength, **Figure 4b** shows the created magnetic forces for push (green curve) versus pull (blue curve). For nanoparticles placed into the middle ear of a human patient, the push system will apply 20× more force than the pull system.

Our magnetic push system, used at a human face-to-ear distance, has successfully delivered particles and drugs into rat inner ears (138). In our experiments, first rats were anesthetized and 300-nm-diameter red-fluorescent magnetic particles (nano-screenMAG-Chitosan, chemicell,

PHYSICS OF MAGNETIC FIELDS AND PARTICLES

The propagation of magnetic fields through space is described by Maxwell's equations (67). Magnetic fields pass virtually unchanged through the human body because the magnetic susceptibility χ of tissue is close to zero ($\chi_{\text{tissue}} \approx 10^{-6}$ – 10^{-4}) (129, 130). By contrast, the iron cores of ferromagnetic particles have magnetic susceptibilities five to seven orders of magnitude higher ($\chi_{\text{magnetite}} \approx 20$) (131–133), which results in strong interactions with an applied magnetic field.

The magnetic force created on a single spherical magnetic particle is given by (134–136)

$$\vec{F}_M = \frac{4\pi a^3}{3} \frac{\mu_0 \chi}{(1 + \chi/3)} \vec{H} \frac{d\vec{H}}{d\vec{x}} = \frac{2\pi a^3}{3} \frac{\mu_0 \chi}{(1 + \chi/3)} \nabla(|\vec{H}|^2), \quad (1)$$

where \vec{H} is the applied magnetic field, μ_0 is the magnetic permeability of vacuum, a is the radius of the particle, $\vec{x} = (x, y, z)$ is its location, and $\nabla = (\frac{\partial}{\partial x}, \frac{\partial}{\partial y}, \frac{\partial}{\partial z})$ is the spatial gradient operator. Thus the force on a magnetic particle scales with its volume ($V = 4\pi a^3/3$). The first relation shows that a spatially varying magnetic field ($d\vec{H}/d\vec{x} \neq 0$) is required to create a magnetic force on the particle. The second relation is equivalent by the chain rule. In it, the gradient operator ∇ points from low to high regions of the magnetic field squared ($|\vec{H}|^2$), which means, as shown schematically in **Figure 3a**, that magnetic particles experience forces from low to high applied magnetic field. The magnetic field is highest closest to a single permanent or electromagnet, and so a single magnet, regardless of its polarity, will always attract ferromagnetic particles.

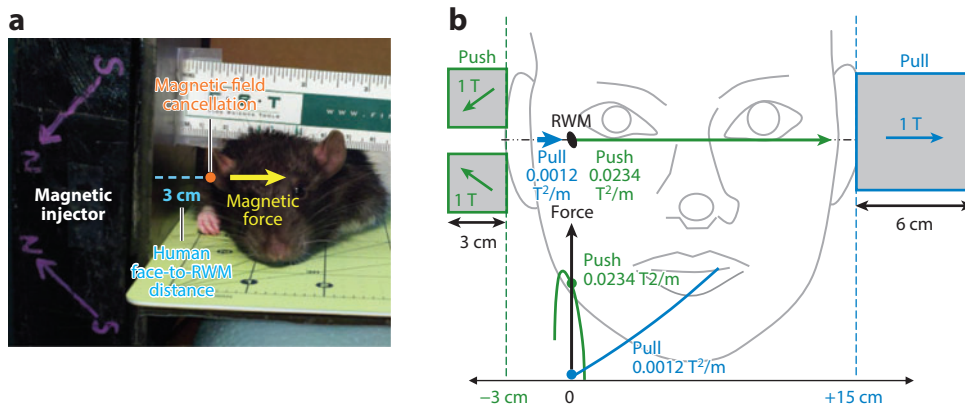


Figure 4

(a) This magnet push system has an internal magnetization strength of approximately ~ 1.5 T and was constructed to our specifications from grade N52 NdFeB magnetic material by Dexter Magnetic Technologies. The device magnetization directions are shown by the purple S \rightarrow N (South to North) markings. The resulting magnetic field cancellation node (orange dot) has been placed just behind the nanoparticles in the middle ear, and it creates an outward magnetic force (yellow arrow) from the middle to the inner ear (138). (b) Push versus pull. Our optimally designed push system operating at a 3-cm distance from the round window membrane (RWM, black oval) applies $20\times$ more force than a comparable pull magnet placed on the opposite side of the head. The force per particle is proportional to the gradient of the magnetic field squared (here, marked in units of T^2/m along the black vertical force axis). The value of ∇H^2 at the RWM is $0.0234 T^2/m$ for the push system versus $0.0012 T^2/m$ for the pull system. Abbreviation: *H*, applied magnetic field; NdFeB, neodymium iron boron. (©2012 IEEE; figure reprinted with permission from 88.)

Berlin, Germany) were deposited by syringe into their middle ears. Then these particles were magnetically pushed into the inner ear by the magnetic system, which was applied for 1 h at a 3-cm magnet-to-inner-ear distance, as shown in **Figure 4a**. Then the rats were euthanized, and their cochleas removed. Isolated cochleas were broken at selected places to remove tissue scrapes, which were examined for the presence or absence of fluorescent nanoparticles. Animals with applied magnetic push had red fluorescence visible in the scrapes, indicating the presence of particles in their cochleas; control animals with particles placed in their middle ear without any magnetic push did not have any cochlear fluorescence (138). Treatment safety was verified by behavioral audiogram studies and by auditory brain-stem response (ABR) recordings (139). Starting 5 days after treatment, we observed nanoparticles in the superior posterior jugular lymph node, which is thought to drain the inner ear, thus suggesting that particles can be cleared from the cochlea.

In subsequent experiments, the chemicell nanoparticles were coated with prednisolone (approximately 0.15 fg per particle) bound reversibly (ionically) to the chitosan particle coating. The amount of drug delivered into the cochlea perilymph was measured by liquid chromatography followed by mass spectrometry in sacrificed animals and was found to be $0.94 \pm 0.1 \mu\text{g/mL}$ 1 h after magnetic injection. In behavioral studies, rats with magnetically injected prednisolone showed recovered hearing after noise trauma, compared with control rats that had free prednisolone deposited into their middle ears according to the current standard of care and still experienced severe hearing loss (A. Sarwar, R. Basiri, M. Ahmed, R. Lee, B. Shapiro & D. Depireux, unpublished manuscript).

3. DRUG DELIVERY TO THE MIDDLE EAR

It is also desirable to better deliver drugs and therapy to the middle ear. Middle ear infections are the leading cause of visits to physicians by children (140–144). In the United States, there are an estimated 15 million cases per year of acute otitis media (AOM) in children younger than five years of age, with associated public health-care costs reaching \$3–5 billion (145). Approximately 20% of patients with AOM develop chronic otitis media with effusion (COME), which is characterized by secretory epithelial metaplasia and the persistence of middle ear effusion, most frequently mucoid (146–148). COME is associated with hearing loss, delayed speech development, cholesteatoma, and the potential for permanent middle ear damage (149, 150).

The standard of care for AOM is usually systemic antibiotic administration (151). Currently, 42% of all antibiotics prescribed in the United States are for the treatment of AOM. This pattern of systemic antibiotic use for AOM has contributed significantly to the appearance of resistant organisms and to an increased incidence of antibiotic-related side effects (145, 152). Although systemic antibiotics may reduce the severity of symptom burden and the duration of AOM in children (153, 154), they have no effect on the clearance of middle ear fluid. There are no effective nonsurgical treatments for COME, nor are there treatments that block the progression of AOM to COME. For this reason, in the United States, the most common pediatric surgical procedure requiring general anesthesia is tympanostomy tube placement for recurrent AOM or COME (155). General anesthesia is required because children will not lie still for a middle ear surgery under topical anesthesia. Thus there is a clear public health need for alternative strategies to treat AOM and COME, not only to minimize side effects and the development of resistant microorganisms, but also to reduce the costly burden and attendant risks of surgical procedures and general anesthesia in children.

In the clinic, there are no effective nonsurgical techniques to direct drugs through the tympanic membrane (eardrum) (156). Researchers have proposed temporarily chemically permeabilizing the tympanic membrane to enable transport of small molecules (157, 158). Khoo et al. (157) investigated a hydrogel loaded with ciprofloxacin and chemical permeation enhancers (bupivacaine, limonene, sodium dodecyl sulfate). The gel would be placed in the patient's outer ear to enhance delivery of the drug through the tympanic membrane and into the middle ear. Khoo and coworkers validated treatment safety *in vivo* by auditory brain response measurements in live chinchillas and showed enhanced drug delivery *ex vivo* across freshly harvested chinchilla tympanic membranes.

Our results indicate that magnetic injection can deliver drugs to the middle ear, without a need for eardrum puncture or permeabilization. Instead of a tympanostomy procedure, the concept is to place drug-coated magnetic particles into the outer ear and then use magnetic push to direct them into the middle ear without any surgery or anesthesia. Using the same magnetic injector shown in **Figure 4a**, now held at the anticipated distance from magnet to middle ear in a child, we were able to direct 100-nm magnetic particles into rat middle ears by first filling the ear canal with a solution of drug-loaded magnetic particles. The amount of drug delivered into the middle ear was still highly variable, ranging from 10 ng to 1 μ g of prednisolone, and research is ongoing to identify causes for and to reduce this variability.

4. THERAPY DELIVERY TO THE EYE

Age-related macular degeneration (AMD), diabetic maculopathy, and retinitis pigmentosa are the most common causes of blindness in the United States (159–161). In late-stage (wet) AMD, there is a proliferation of abnormal and leaky blood vessels behind the retina. They release blood and fluid,

and the resulting forces can lead to swelling, damage, scarring, and detachment of the pigment epithelium in the retina (162, 163). The standard of care for wet AMD is multiple syringe injections of anti-vascular endothelial growth factor (VEGF) monoclonal antibody fragments (e.g., Lucentis) into the eye (as VEGF promotes the growth of new vessels) (164, 165), as well as laser treatment of select areas of the retina (photodynamic therapy) (35, 166) and laser surgery to destroy some of the abnormal blood vessels (photocoagulation therapy) (167).

Diabetic maculopathy occurs when abnormal blood vessels due to diabetes cause damage at the highly pigmented yellow spot (macula lutea in Latin), at the center of the retina, responsible for central vision (168). Diabetic maculopathy is also currently treated by anti-VEGF injection or injection of steroids into the eye (169).

Retinitis pigmentosa is an inherited degenerative eye disease caused by progressive deterioration of rods and cones or the retinal pigment epithelium (RPE) (170, 171). There is no known cure, but the disease can be slowed by the daily intake of vitamin A in some patients (172). Emerging treatments include surgical implantation of cells transfected with human ciliary neurotrophic factor (CNTF) genes (173); topical application (eye drops) of insulin, insulin-like growth factor (IGF)-1, and chlorin e6 (174); and viral-vector delivery of the *RPE65* gene (for creation of a RPE-specific protein) by injection between the RPE cell layer and the photoreceptor layer (175–178).

Other causes of blindness include central retinal vein occlusion and endophthalmitis. Central retinal vein occlusion refers to a blockage of the vein that drains the blood from the eye, and it is a condition that can lead to severe damage to the retina and blindness (179, 180). Treatment consists of injection of anti-VEGF drugs, intravitreal placement of a biodegradable steroid-releasing implant (Ozurdex, <http://www.ozurdex.com/AboutOzurdex.aspx>), or panretinal laser photocoagulation (181–185).

Endophthalmitis, the infection and inflammation of the intravitreal cavity, is a possible complication of all intraocular surgeries, particularly cataract surgeries, and can lead to loss of vision and loss of the eye itself (165, 186–189). Endophthalmitis is also treated by injection of drugs into the eye, in this case antibiotics (165, 190, 191). For most of the conditions above, the need to deliver drugs to the retina and the cumulative risks of doing so invasively (via syringe injections) highlight the need for more effective but minimally invasive eye drug delivery methods.

The eye consists of several compartments (**Figure 5**) and can be loosely divided into posterior and anterior regions (192, 193). To reach these compartments, therapies must overcome several biological barriers, either from cellular membranes (cornea, sclera, retina, or blood–retinal barriers), active fluid transport (choroidal blood flow, conjunctival blood flow, lymphatic drainage, and tear dilution), or active transport pumps within cellular membranes (192, 193). Based upon the chosen drug delivery route (topical, oral, intravitreal, intracameral, subconjunctival, subtenon, retrobulbar, or posterior juxtасleral), all or some of these biological barriers will be present and must be addressed. For retinal therapies, systemic administrations are an attractive noninvasive option, but deep permeation into the retina is limited by the blood–retinal barrier (192, 193). Subretinal injections have been used to deliver therapies to the retinal lining, but this clinical procedure carries risks of ocular infection and retinal detachment (194–196). The rate of complications per intraocular drug delivery procedure into a single eye is estimated to be 0.2% for endophthalmitis and 0.05% for retinal detachments (195, 197).

Nonmagnetic genetic therapy systems that rely on diffusion to transport therapies from the sclera to the retina have been explored. These systems include application of ophthalmic gels, such as gellan gum (198) sold as Timoptic-XE[®] by Merck & Co. Inc. (Whitehouse Station, NJ) and chitosan gels (199) being developed by PhotoBioMed Corp. (Dallas, TX). There are also treatments that attempt to increase sclera permeability by prodrug design or by increasing solubility. The prodrug nepafenac manufactured by Alcon has been shown to improve permeability

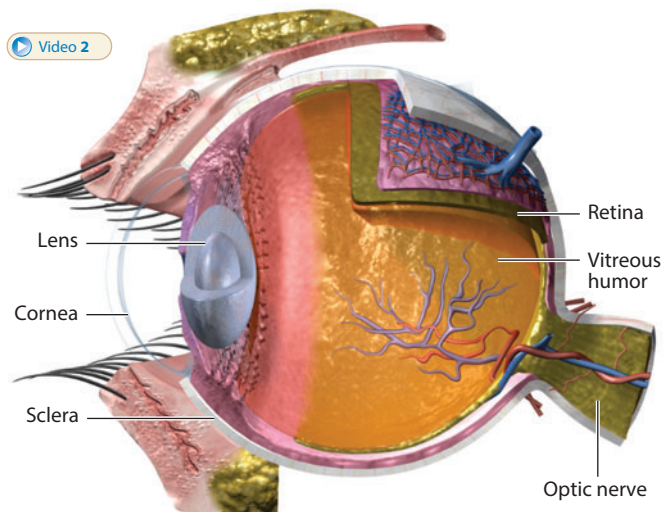


Figure 5

The anatomy of the human eye. **Video 2** shows an animation of this anatomy. (Figure adapted with permission from 3D4Medical.com, ©2013.)

(200). The recent survey article by Weiner & Gilger (201) provides an excellent overview of the currently available techniques for drug delivery into the eye.

Magnetically manipulated nanoparticles for therapy delivery to the eye have been tested in animal experiments. Luty and coworkers (202, 203) have developed magnetic nanoparticles conjugated with bare DNA to treat reactive oxygen degeneration in the retinal layer of rabbits. Dengler et al. (204) systemically administered magnetic cobalt nanoparticles into the tail veins of mice and placed an external cylindrical magnet in front of the eyes. The magnet was held for 30 min, and then the animal was sacrificed and retinal whole mounts were prepared and examined. Many scattered nanoparticles were observed in retinas where the magnet was applied, compared with few observed particles for control animals (no applied magnet). The long-term toxicity of nanoparticles in the eye was investigated by Raju et al. (205), and these authors found that particles were generally well tolerated by ocular tissues.

Magnetic fields have also been used to direct mesenchymal stem cells to the retina. Stem cells have the potential to regenerate retina tissue or provide sustained release of a range of neuroprotective and anti-inflammatory molecules. Yanai et al. (32) isolated mesenchymal stem cells from rat bone marrow and cultured them with 200-nm-diameter superparamagnetic iron oxide nanoparticles (SPIONs). Stem cells containing SPIONs were then administered to rats either by direct injection into the vitreous cavity of one eye or via intravenous tail vein injection. In both cases, a 3-mm-diameter, 1.5-mm-thick gold-plated NdFeB disc magnet was placed within the orbit but outside of the eye in test rats; in control rats, no magnet was used. **Figure 6** shows results reproduced from this study (32). The disc magnet significantly increased stem cells delivered to the upper retinal hemisphere for intravitreal injection (**Figure 6b** versus **Figure 6a**). The cells aggregated in a circle corresponding to the circular edge of the magnet, where the magnetic intensity was highest (at the magnet corners, as in **Figure 3**). Stem cell delivery to the upper retinal hemisphere was also increased for intravenous administration (**Figure 6d** and **Figure 6f** versus **Figure 6c** and **Figure 6e**, respectively), with a 10-fold increase observed. Moreover, in animals without an applied magnet, stem cells were observed only on the retinal surface in retinal cryosections. However, for animals with the implanted disc magnet, stem cells were also present

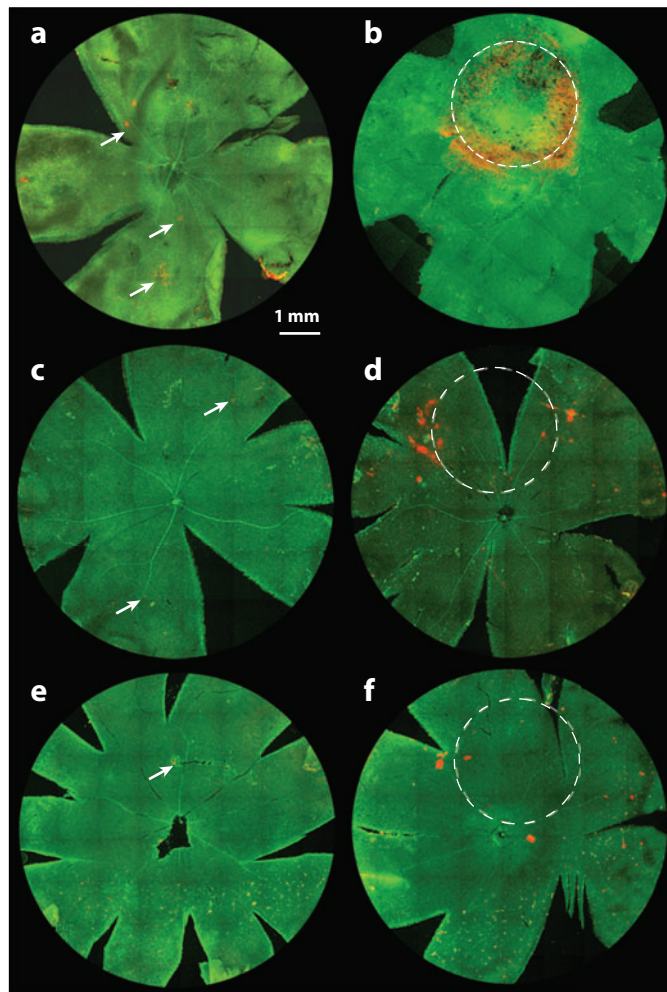


Figure 6

Flat-mount images of rat retinas (*a,c,e*) in control animals and (*b,d,f*) after magnetic targeting of stem cells. Arrows indicate small areas of magnetic mesenchymal stem cells in the retinas without a magnet applied. The dashed white circle shows the position of the orbital disk magnet. Stem cells have been labeled with Qtracker 655 and appear red/orange in the image. (Figure courtesy of Urs Hafeli and reproduced with permission, *Cell Transplantation*, ISSN:0963-6897, DOI:<http://dx.doi.org/10.3727/096368911X627435>, volume 21, issue 6, figure 3, p. 1142, ©2012 Cognizant Comm. Corp.).

in the inner and outer retina—a benefit for treatment of AMD and retinitis pigmentosa, which particularly affect the outer retina (206–208).

The same push system that was used to magnetically inject therapy into the inner and middle ear has also shown initial success in directing particles topically into the eye, without a need to pierce the eye with a syringe. In preliminary rat experiments, we employed a 1-cm contact lens with 40 μL of 100-nm-diameter starch-coated magnetic nanoparticles within the well of the contact lens. The lens was placed on the eye, and the magnetic push system illustrated in **Figure 4a** was aligned to push the magnetic particles to the retina for 1 h, at which point the animal was sacrificed and its eye excised. The presence of nanoparticles in the eye was verified by histology (with Perls'

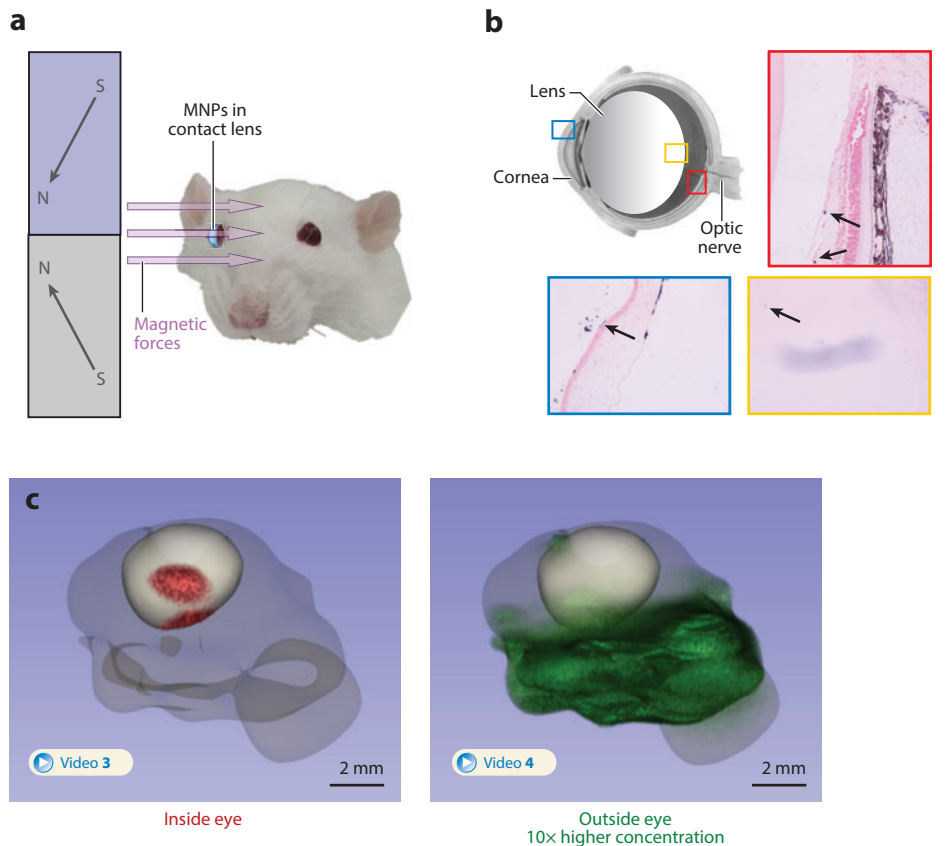


Figure 7

Noninvasive magnetic delivery of particles into the eye. (a) Schematic of the rat experiment. A contact lens containing magnetic nanoparticles (MNPs) is placed on the eye. Magnetic forces push the particles into the eye. (b) Histological sections of MNPs within a single rat eye. Particles (arrows) are stained by Perls' Prussian blue and are seen as dark blue against the nuclear fast red counterstain. A schematic of the eye with corresponding color-coded boxes shows the approximate spatial location of each histological slice. (c) Three-dimensional distribution of the fluorescent MNPs within a single rat eye [shown in red for particles that were found inside the eye (left) and in green for particles that remained outside the eye (right)]. **Video 3** and **Video 4** show animations of the illustrations on the left and right of this panel, respectively.

Prussian blue stain). We measured the three-dimensional (3D) distribution of the particles (shown in **Figure 7c**) using an automated 3D fluorescence imaging cryostat system (209, 210). We are working to improve the delivery efficiency, and the particles are now being functionalized with heparin and adeno-associated viral vectors for potential treatment of Leber congenital amaurosis.

An electromagnet system that shapes magnetic fields to precisely control a microrobot in the eye is being developed by Nelson's group (211–214). Their goal is to enable delivery of drugs to specific locations on the retina, as well as to improve delicate retinal procedures such as retinal-vein cannulation (the injection of clot-busting drugs into small veins). Retinal-vein cannulation requires surgical manipulation at the limit of what trained eye surgeons can achieve (215–217). The group's OctoMag system consists of eight electromagnets arranged in a hemisphere around the

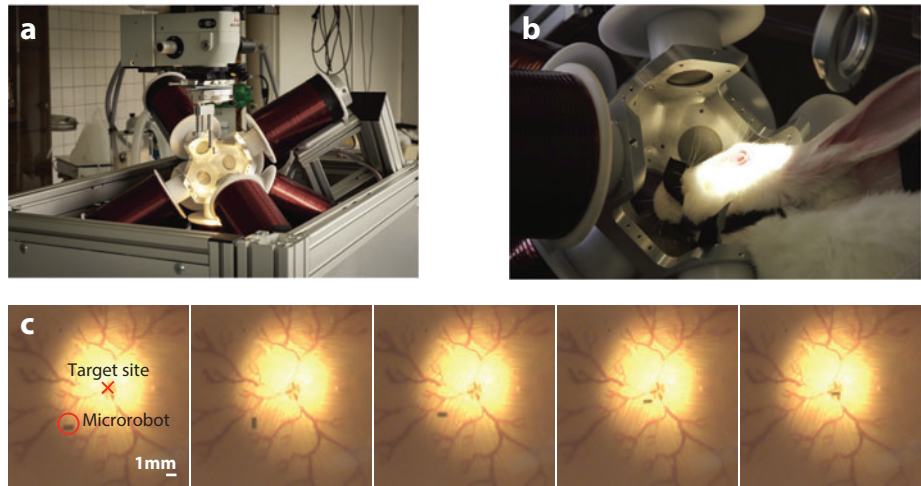


Figure 8

Shaping a magnetic field in space and time to manipulate a microrobot inside the eye. (a) The eight-electromagnet OctoMag system. (b) An anesthetized rabbit placed with its eye in the OctoMag workspace. (c) Manipulation of the microrobot to the retina macula in an eye phantom. (Figure courtesy of Bradley Nelson and reproduced with permission from 211 and 213, ©2013 Investigative Ophthalmology.)

eye to be treated (**Figure 8**). They can apply up to 40-mT shaped magnetic fields with gradients of up to 1 T/m.

In their animal experiments, Nelson's group injected a soft magnetic hollow cylinder (the microrobot, which measures 285 μm in outer diameter, 125 μm in inner diameter, and 1.8 mm in length) into a rabbit eye using a 23 gauge needle. This microrobot currently features a drug release reservoir, and mechanical components (such as needles or hooks for surgical procedures) are planned for next-generation devices. In the rabbit eye, the location and orientation of the microrobot were observed in real time by a microscope and camera and were either displayed on-screen for a human user or tracked by a computer-imaging algorithm for closed-loop automated control. The group developed a physics-based mathematical model that describes the magnetic field, force, and torque on the robot. The model provided a known precomputed mapping from the eight electromagnet currents to the resulting force and torque produced on the microrobot, at any robot location and orientation within the eye. Least-squares (pseudoinverse) inversion was used to invert this model and find the electromagnet currents at each time to produce the user-requested or computer-commanded robot motion, and these currents were then applied to the eight electromagnets to manipulate the robot to the desired retina locations. After the procedure, the robot was removed from the eye by guiding it to a magnetic tool (a needle with a magnetic wire inserted into it) and pulling it out of the rabbit eye. **Figure 8** shows the OctoMag system and manipulation of a microrobot to the retina macula inside an eye phantom (211–214).

5. NEEDS AND FUTURE DIRECTIONS

For magnetic-therapy targeting, it is not enough to have biocompatible drug-eluting magnetic carriers or living therapeutic stem cells safely loaded with magnetic nanoparticles; magnet systems that effectively direct such magnetic constructs to disease locations in human patients are also needed. A single magnet can perform only a limited function: It can only attract magnetic

constructs (see Sidebar). Multiple magnets, working in concert, are required to inject therapy or to precisely manipulate it inside the body.

To rationally design such multimagnet systems, we need mathematical models. In order to determine where to place magnets, their size and strength, and when to turn them on and off to direct magnetic constructs to clinical targets, we need a quantitative description of how magnetized materials will move under applied magnetic fields. The necessary mathematical description can be split into two parts: (a) quantifying the magnetic forces created on magnetic materials and (b) quantifying *in vivo* resistance to the motion of magnetic materials in tissue, across membranes, and through bodily fluids. The first part can be addressed readily enough with standard physics. As discussed in the Sidebar, classical physics can be used to quantify the force on single nanoparticles, and there are results and theories both for nanoparticles that have agglomerated together and for carriers with nonspherical shapes (218–220).

The second part—mathematically describing the resistance forces that magnetic particles and cells encounter *in vivo*—is more difficult, is variable (from tissue to tissue, from animal to animal), and is not well understood. In two studies (221, 222), we first examined how blood-flow viscous drag forces on particles compete against magnetic forces and then summarized our findings in a nondimensional design space figure (figure 11 in 221 and figure 5 in 222) that predicted when applied magnetic fields were able to capture particles of different sizes against blood flow in different vessels. Our particle-capture predictions matched available *in vitro* and *in vivo* experimental data, but tissue (vessel endothelium) resistance to particle motion was simplistically represented by a single diffusion coefficient. In subsequent work (223), we analyzed how particles of different sizes might move through tissue under a magnetic field using two common mathematical models of tissue resistance—the Renkin pore model (224) and the fiber-matrix model (225). The models predicted a trade-off: If the particles are too small, they do not experience enough magnetic force to move effectively through tissue; if the particles are too large, they experience too much tissue resistance to move effectively. Thus there was a particle-size sweet spot for best motion, and that optimal size depends on tissue properties and the strength of the magnetic gradient that can be applied. **Figure 9** shows the effectiveness of magnetically induced particle motion (as compared with diffusion only) for a fixed applied magnetic gradient. Depending on tissue properties (the vertical axis), there is an intermediate particle radius (the yellow/red regions) at which magnetic forces provide a benefit. The predictions of this figure have not yet been tested against experiments, and more generally, a great deal of research remains to be done to understand how tissue properties influence particle motion. In particular, for ears and eyes, we do not yet understand the resistance forces that epithelial and connective tissues apply to magnetic particles as they traverse the eardrum, window membranes, or the eye sclera.

To date, researchers have essentially used a good understanding of magnetic forces (the first part) to correct for our poor understanding of *in vivo* resistance forces (the second part). For magnetic injection into the middle and inner ear, we shaped magnetic fields to maximize the force per particle at tympanic and window membranes (136) so as to increase particle penetration through these membranes. We did so without understanding the details of membrane resistance to particle transport. Likewise, for manipulation of the eye microrobot, Nelson's group first considered only the magnetic portion of the forces and torques they apply and used image-guided feedback control to correct for the effects of fluid resistance to robot motion (211). It was only after an additional three years of research that they first reported on the resistance properties of the vitreous humor in live rabbits (213).

To improve magnetic targeting, as a community we must better understand the second part: the *in vivo* resistance to magnetically induced particle and cell motion, in bodily fluids and tissues, and across membranes. In our lab, we have an ongoing program to systematically measure and

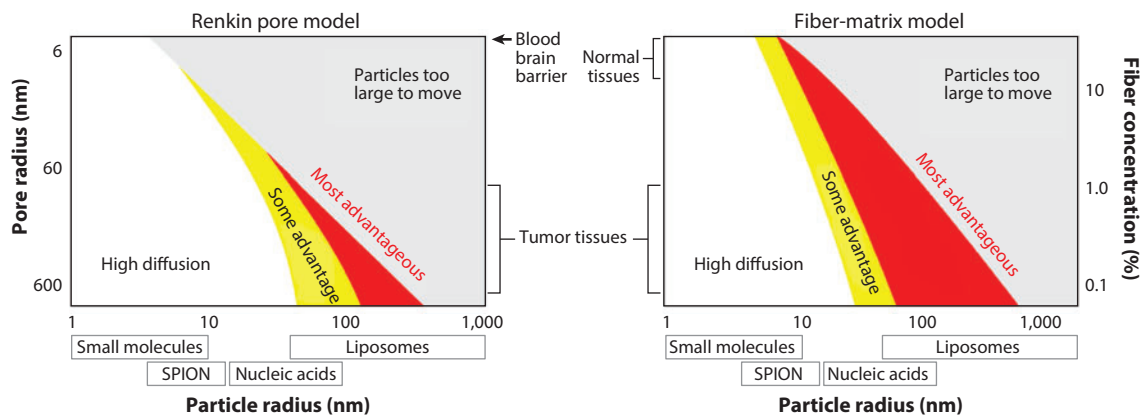


Figure 9

A map of when magnetic forces are beneficial in moving particles through tissue, according to two tissue resistance models: the Renkin and the fiber-matrix models (224, 225). The horizontal axis represents particle size (small particles have high diffusion: *white region on the left*). The vertical axis represents tissue properties (normal tissue at the top has an increased resistance to particle motion compared with tumor tissue at the bottom). Particles that are too large cannot move even when a magnetic field is applied (*gray region on the right*); small particles already diffuse effectively and so do not benefit from magnetic forces. Hence particles of intermediate size (*yellow and red regions*) benefit from the applied magnetic field (here, a 2.5-T magnet placed 11 cm away from the tissue). For analysis details, please see 223. Note the log scale for the horizontal axis. Abbreviation: SPION, superparamagnetic iron oxide nanoparticle. (Figure adapted with permission from 223.)

quantitatively describe the transport of magnetic particles through blood and tissue. These data will be used to improve our mathematical models (221–223), to extend them to nonspherical particles and to cells that contain magnetic materials. To that end, we have initiated an effort to systematically measure and quantify the transport of magnet particles and cells through freshly excised tissues (liver, brain, kidney, ear, and eye tissues) for different particle types (size, shape, and coating), as well as for live cells that contain particles. We apply known magnetic forces and then measure the resulting distribution of particles and labeled cells throughout the tissue (209, 226). The goal is to begin to understand and quantify tissue resistance forces. It is our hope that other magnetic drug targeting groups will join this effort.

There is also a need for more precise magnetic control of the spatial distribution of therapy. For the inner ear, not only do we want to inject therapy, but we also want to ensure that we are dosing the entire cochlea surface fairly uniformly with particles (and thus drugs). For the eye, the goal is to noninvasively direct therapy only to the diseased portions of the retina. This requires more than just magnetic injection of drug-eluting nanoparticles into an anatomical space and more than precision control of a single drug-releasing micro-object; it requires magnetic shaping of the spatial distribution of therapy *in vivo*. Ear anatomical data (Figure 1b) and mathematical models of pharmacokinetics along the cochlea spiral (see <http://oto2.wustl.edu/cochlea/> and 227) are allowing us to better select magnetic forces for the ear. We are shaping the magnetic injection forces so that they always have a component up the cochlea spiral, in order to direct and deposit drug-eluting particles throughout the cochlea. We are also attempting to focus a distributed fluid of magnetic particles to deep internal targets by coordinated control of multiple external magnets (88). However, this effort is still at the numerical simulation stage, and its success hinges on effective mathematical descriptions of tissue resistance to nanoparticle motion.

Truly deep magnetic targeting, reaching targets that are beyond the 2–5-cm ear and eye target depths discussed above, will likely require new magnetic carrier choices and designs. Optimal design of external magnets can provide an order-of-magnitude increase in applied forces (e.g.,

Figure 4b). Optimally selecting the properties of the in vivo magnetic constructs can likely provide additional order-of-magnitude improvements. The magnetic force applied on a nanoparticle scales with the volume of that particle (see Sidebar). Viscous resistance in blood (Stokes' drag) scales with particle radius (228). Thus, increasing the particle size by a factor of 10 changes the ratio of magnetic to resistance forces, in blood, by a factor of 100. Tissue resistance can include viscous effects (229, 230), fiber network and pore resistance to motion (224, 225), and particle-to-tissue adhesion (231, 232). The latter likely scales with particle surface area and, we have found, can be highly dependent on particle coatings (226). Thus, changing particle size and coating can also dramatically change the balance of forces in tissue. In addition, there are particle shape and flexibility parameters (e.g., flexible tubes versus hard spheres), as well as particle agglomeration, and then there are live cells whose shape can deform as they move through tissue and that can be loaded with hundreds to thousands of magnetic nanoparticles each. All of these factors (particle size, shape, coating, and agglomeration, as well as cell type, magnetic loading, and deformation) can likely substantially affect motion through tissue in complex ways. To improve magnetic targeting, the field needs a body of work that measures, quantifies, analyzes, and begins to understand these factors, first in vitro and then in vivo. This knowledge should then drive the choice, design, and implementation of next-generation magnetic constructs.

Deep targeting also requires improved imaging of magnetic constructs, which is an active research area (59, 233–236). To magnetically focus particles to a deep tumor will require an imaging system that can see the particles deep in vivo, in real time, so that magnets outside the patient can be appropriately actuated in response, to direct the particles from where they are to where they should be. MRI can identify large concentrations of magnetic nanoparticles owing to their extinction of the magnetic resonance signal (negative lack-of-signal imaging) (45, 235). Recently, Kim et al. (235) showed that MRI sequences can be modified to positively visualize specifically designed magnetic particles. This increased imaging contrast and allowed quantification of particle concentrations. Magnetic particle imaging (MPI) (88, 234, 237, 238) is another emerging imaging modality that also exploits the physical properties of magnetic particles and selectively images them. This technique has recently been overlaid with MRI to visualize the flow of red blood cells loaded with magnetic particles through the heart of a mouse (238). Overall, there is a broad need to develop these and other imaging methods, to improve their resolution and speed, and to interleave them with magnetic control to achieve deep and precise magnetic targeting.

In closing, designing and implementing effective magnetic delivery systems will require collaboration between engineers, physicists, and mathematicians (who understand how to design and build systems) and clinicians, biologists, biochemists, and nanotechnologists (who can help unravel how drugs and nanotherapeutics move inside the body). We have focused this article on two shallow (≤ 5 cm deep) clinical targets—the ear and the eye—for which the action of a single external magnet is not sufficient. In these two cases, shaping of the magnetic field, in time and space, by multiple magnets working in concert, is allowing minimally invasive delivery and precision control of therapy to middle-ear, cochlea, and retina targets.

DISCLOSURE STATEMENT

B.S., A.N., and D.A.D. have an ownership stake in Otomagnetics LLC, a company that is commercializing magnetic delivery to ears and eyes.

ACKNOWLEDGMENTS

A larger number of colleagues and collaborators have made this article possible. The authors thank Mohammed Ahmed, Behnam Badie, Reza Basiri, Christian Bergemann, Jacob Berlin, Steven

Bernstein, David Beylin, Kenneth Dormer, Urs Hafeli, Andreas Lübbe, Arkadi Nemirovski, Bradley Nelson, Isaac Rutel, Alec Salt, Simone Schürle, Franziska Ullrich, and Irving Weinberg. Funding from the National Institutes of Health (NIH), the National Science Foundation (NSF), and the CDMRP, as well as the Technology Development Corporation (TEDCO) and the Maryland Industrial Partnerships (MIPS) agencies in the State of Maryland and Action on Hearing Loss in the United Kingdom, is gratefully acknowledged.

LITERATURE CITED

1. Reszka R, Beck P, Fichtner I, Hentschel M, Richter J, Kreuter J. 1997. Body distribution of free, liposomal and nanoparticle-associated mitoxantrone in B16-melanoma-bearing mice. *J. Pharmacol. Exp. Ther.* 280(1):232–37
2. Davies NM. 2000. Biopharmaceutical considerations in topical ocular drug delivery. *Clin. Exp. Pharmacol. Physiol.* 27(7):558–62
3. Parnes LS, Sun A-H, Freeman DJ. 1999. Corticosteroid pharmacokinetics in the inner ear fluids: an animal study followed by clinical application. *Laryngoscope* 109(S91):1–17
4. Juhn SK, Hunter BA, Odland RM. 2001. Blood-labyrinth barrier and fluid dynamics of the inner ear. *Int. Tinnitus J.* 7(2):72–83
5. Inamura N, Salt AN. 1992. Permeability changes of the blood-labyrinth barrier measured in vivo during experimental treatments. *Hear. Res.* 61(1–2):12–18
6. Orekhova NM, Akchurin RS, Belyaev AA, Smirnov MD, Ragimov SE, Orekhov AN. 1990. Local prevention of thrombosis in animal arteries by means of magnetic targeting of aspirin-loaded red cells. *Thromb. Res.* 57(4):611–16
7. Lübbe AS, Bergemann C, Riess H, Schriever F, Reichardt P, et al. 1996. Clinical experiences with magnetic drug targeting: a Phase I study with 4'-epidoxorubicin in 14 patients with advanced solid tumors. *Cancer Res.* 56(20):4686–93
8. Shinkai M. 2002. Functional magnetic particles for medical application. *J. Biosci. Bioeng.* 94(6):606–13
9. Alexiou C, Jurgons R, Schmid RJ, Bergemann C, Henke J, et al. 2003. Magnetic drug targeting—biodistribution of the magnetic carrier and the chemotherapeutic agent mitoxantrone after locoregional cancer treatment. *J. Drug Target.* 11(3):139–49
10. Wilson MW, Kerlan RK, Fidelman NA, Venook AP, LaBerge JM, et al. 2004. Hepatocellular carcinoma: regional therapy with a magnetic targeted carrier bound to doxorubicin in a dual MR imaging/conventional angiography suite—initial experience with four patients. *Radiology* 230(1):287–93
11. Koda J, Venook A, Walsler E, Goodwin S. 2002. A multicenter, phase I/II trial of hepatic intra-arterial delivery of doxorubicin hydrochloride adsorbed to magnetic targeted carriers in patients with hepatocellular carcinoma. *Eur. J. Cancer* 38(Suppl. 7):S18
12. Johannsen M, Gneveckow U, Eckelt L, Feussner A, Waldöfner N, et al. 2005. Clinical hyperthermia of prostate cancer using magnetic nanoparticles: presentation of a new interstitial technique. *Int. J. Hyperthermia* 21(7):637–47
13. Dobson J. 2006. Magnetic micro- and nano-particle-based targeting for drug and gene delivery. *Nanomedicine* 1(1):31–37
14. Maier-Hauff K, Ulrich F, Nestler D, Niehoff H, Wust P, et al. 2010. Efficacy and safety of intratumoral thermotherapy using magnetic iron-oxide nanoparticles combined with external beam radiotherapy on patients with recurrent glioblastoma multiforme. *J. Neuro-Oncol.* 103(2):317–24
15. Morishita N, Nakagami H, Morishita R, Takeda S, Mishima F. 2005. Magnetic nanoparticles with surface modification enhanced gene delivery of HVJ-E vector. *Biochem. Biophys. Res. Commun.* 334(4):1121–26
16. Mah C, Fraites TJ, Zolotukhin I, Song S, Flotte TR, et al. 2002. Improved method of recombinant AAV2 delivery for systemic targeted gene therapy. *Mol. Ther.* 6(1):106–12
17. Lu J, Ma S, Sun J, Xia C, Liu C, et al. 2009. Manganese ferrite nanoparticle micellar nanocomposites as MRI contrast agent for liver imaging. *Biomaterials* 30(15):2919–28

18. Kubo T, Sugita T, Shimose S, Nitta Y, Ikuta Y, Murakami T. 2001. Targeted systemic chemotherapy using magnetic liposomes with incorporated adriamycin for osteosarcoma in hamsters. *Int. J. Oncol.* 18(1):121–26
19. Wu J, Leong-Poi H, Bin J, Yang L, Liao Y, et al. 2011. Efficacy of contrast-enhanced US and magnetic microbubbles targeted to vascular cell adhesion molecule-1 for molecular imaging of atherosclerosis. *Radiology* 260(2):463–71
20. Kong SD, Lee J, Ramachandran S, Eliceiri BP, Shubayev VI, et al. 2012. Magnetic targeting of nanoparticles across the intact blood–brain barrier. *J. Control. Release* 164(1):49–57
21. Mihaiescu DE, Buteică AS, Neamțu J, Istrati D, Mîndrilă I. 2013. Fe₃O₄/Salicylic acid nanoparticles behavior on chick CAM vasculature. *J. Nanopart. Res.* 15:1857
22. Stanley SA, Gagner JE, Damanpour S, Yoshida M, Dordick JS, Friedman JM. 2012. Radio-wave heating of iron oxide nanoparticles can regulate plasma glucose in mice. *Science* 336(6081):604–8
23. Cho MH, Lee EJ, Son M, Lee J-H, Yoo D, et al. 2012. A magnetic switch for the control of cell death signalling in in vitro and in vivo systems. *Nat. Mater.* 11:1038–43
24. Gao F, Kar S, Zhang J, Qiu B, Walczak P, et al. 2007. MRI of intravenously injected bone marrow cells homing to the site of injured arteries. *NMR Biomed.* 20(7):673–81
25. Pislaru SV, Harbuzariu A, Gulati R, Witt T, Sandhu NP, et al. 2006. Magnetically targeted endothelial cell localization in stented vessels. *J. Am. Coll. Cardiol.* 48(9):1839–45
26. Gazeau F, Wilhelm C. 2010. Magnetic labeling, imaging and manipulation of endothelial progenitor cells using iron oxide nanoparticles. *Future Med. Chem.* 2(3):397–408
27. Pawelczyk E, Jordan EK, Balakumaran A, Chaudhry A, Gormley N, et al. 2009. In vivo transfer of intracellular labels from locally implanted bone marrow stromal cells to resident tissue macrophages. *PLoS ONE* 4(8):e6712
28. Arbab AS, Jordan EK, Wilson LB, Yocum GT, Lewis BK, Frank JA. 2004. In vivo trafficking and targeted delivery of magnetically labeled stem cells. *Hum. Gene Ther.* 15(4):351–60
29. Chen J, Jia Z-Y, Ma Z-L, Wang Y-Y, Teng G-J. 2011. In vivo serial MR imaging of magnetically labeled endothelial progenitor cells homing to the endothelium injured artery in mice. *PLoS ONE* 6(6):e20790
30. Qiu B, Gao F, Walczak P, Zhang J, Kar S, et al. 2007. In vivo MR imaging of bone marrow cells trafficking to atherosclerotic plaques. *J. Magn. Reson. Imaging* 26(2):339–43
31. Polyak B, Fishbein I, Chorny M, Alferiev I, Williams D, et al. 2008. High field gradient targeting of magnetic nanoparticle-loaded endothelial cells to the surfaces of steel stents. *Proc. Natl. Acad. Sci. USA* 105(2):698–703
32. Yanai A, Häfeli UO, Metcalfe AL, Soema P, Addo L, et al. 2012. Focused magnetic stem cell targeting to the retina using superparamagnetic iron oxide nanoparticles. *Cell Transplant.* 21(6):1137–48
33. Hofmann A, Wenzel D, Becher UM, Freitag DF, Klein AM, et al. 2009. Combined targeting of lentiviral vectors and positioning of transduced cells by magnetic nanoparticles. *Proc. Natl. Acad. Sci. USA* 106(1):44–49
34. Chaudeurge A, Wilhelm C, Chen-Tournoux A, Farahmand P, Bellamy V, et al. 2012. Can magnetic targeting of magnetically labeled circulating cells optimize intramyocardial cell retention? *Cell Transplant.* 21(4):679–91
35. Dougherty TJ, Gomer CJ, Jori G, Kessel D, Korbelik M, et al. 1998. Photodynamic therapy. *J. Natl. Cancer Inst.* 90(12):889–905
36. Barry BW. 2001. Novel mechanisms and devices to enable successful transdermal drug delivery. *Eur. J. Pharm. Sci.* 14(2):101–14
37. Denet AR, Vanbever R, Preat V. 2004. Skin electroporation for transdermal and topical delivery. *Adv. Drug Deliv. Rev.* 56(5):659–74
38. Pitt WG, Hussein GA, Staples BJ. 2004. Ultrasonic drug delivery—a general review. *Expert Opin. Drug Deliv.* 1(1):37–56
39. Gao Z-G, Fain HD, Rapoport N. 2005. Controlled and targeted tumor chemotherapy by micellar-encapsulated drug and ultrasound. *J. Control. Release* 102(1):203–22
40. Allen ED, Burdette JH. 2001. *Questions and Answers in MRI*. St. Louis, MO: Mosby. 2nd ed.

41. Schenck JF. 2000. Safety of strong, static magnetic fields. *J. Magn. Reson. Imaging* 12(1):2–19
42. Schaefer DJ, Bourland JD, Nyenhuis JA. 2000. Review of patient safety in time-varying gradient fields. *J. Magn. Reson. Imaging* 12(1):20–29
43. Andersen E. 2007. Magnetic resonance imaging—safety and health issues. *AAOHN J.* 55(4):137–39
44. Kirui DK, Khalidov I, Wang Y, Batt CA. 2013. Targeted near-IR hybrid magnetic nanoparticles for in vivo cancer therapy and imaging. *Nanomed.: Nanotechnol. Biol. Med.* 9(5):702–11
45. Lemke A, Sander B, Luebke A, Riess H, Hosten N, Felix R. 1996. MR imaging after magnetic drug targeting in patients with soft-tissue tumors. *Radiology* 201:1421
46. Johannsen M, Gneveckow U, Thiesen B, Taymoorian K, Cho CH, et al. 2007. Thermo-therapy of prostate cancer using magnetic nanoparticles: feasibility, imaging, and three-dimensional temperature distribution. *Eur. Urol.* 52(6):1653–61
47. Lemke AJ, Von Pilsach MIS, Lübke A, Bergemann C, Riess H, Felix R. 2004. MRI after magnetic drug targeting in patients with advanced solid malignant tumors. *Eur. Radiol.* 14(11):1949–55
48. Widder KJ, Morris RM, Poore G, Howard DP, Senyei AE. 1981. Tumor remission in Yoshida sarcoma-bearing rats by selective targeting of magnetic albumin microspheres containing doxorubicin. *Proc. Natl. Acad. Sci. USA* 78(1):579–81
49. Pulfer SK, Gallo JM. 1998. Enhanced brain tumor selectivity of cationic magnetic polysaccharide microspheres. *J. Drug Target.* 6(3):215–27
50. Krukemeyer MG, Krenn V, Jakobs M, Wagner W. 2012. Mitoxantrone-iron oxide biodistribution in blood, tumor, spleen, and liver—magnetic nanoparticles in cancer treatment. *J. Surg. Res.* 175(1):35–43
51. Pouponneau P, Leroux J-C, Soulez G, Gaboury L, Martel S. 2011. Co-encapsulation of magnetic nanoparticles and doxorubicin into biodegradable microcarriers for deep tissue targeting by vascular MRI navigation. *Biomaterials* 32(13):3481–86
52. Raut SL, Kirthivasan B, Bommana MM, Squillante E, Sadoqi M. 2010. The formulation, characterization and in vivo evaluation of a magnetic carrier for brain delivery of NIR dye. *Nanotechnology* 21(39):395102
53. Pouponneau P, Leroux J-C, Martel S. 2009. Magnetic nanoparticles encapsulated into biodegradable microparticles steered with an upgraded magnetic resonance imaging system for tumor chemoembolization. *Biomaterials* 30(31):6327–32
54. Liu H-L, Hua M-Y, Yang H-W, Huang C-Y, Chu P-C, et al. 2010. Magnetic resonance monitoring of focused ultrasound/magnetic nanoparticle targeting delivery of therapeutic agents to the brain. *Proc. Natl. Acad. Sci. USA* 107(34):15205–10
55. Tietze R, Jurgons R, Lyer S, Schreiber E, Wiekhorst F, et al. 2009. Quantification of drug-loaded magnetic nanoparticles in rabbit liver and tumor after in vivo administration. *J. Magn. Magn. Mater.* 321(10):1465–68
56. Alexiou C, Jurgons R, Schmid R, Hilpert A, Bergemann C, et al. 2005. In vitro and in vivo investigations of targeted chemotherapy with magnetic nanoparticles. *J. Magn. Magn. Mater.* 293(1):389–93
57. Schulze K, Koch A, Schopf B, Petri A, Steitz B, et al. 2005. Intraarticular application of superparamagnetic nanoparticles and their uptake by synovial membrane—an experimental study in sheep. *J. Magn. Magn. Mater.* 293(1):419–32
58. Forbes ZG, Yellen BB, Halverson DS, Fridman G, Barbee KA, Friedman G. 2008. Validation of high gradient magnetic field based drug delivery to magnetizable implants under flow. *IEEE Trans. Biomed. Eng.* 55(2):643–49
59. Chertok B, Moffat BA, David AE, Yu F, Bergemann C, et al. 2008. Iron oxide nanoparticles as a drug delivery vehicle for MRI monitored magnetic targeting of brain tumors. *Biomaterials* 29(4):487–96
60. Dames P, Gleich B, Flemmer A, Hajek K, Seidl N, et al. 2007. Targeted delivery of magnetic aerosol droplets to the lung. *Nat. Nano* 2(8):495–99
61. Lee J-H, Huh Y-M, Jun Y, Seo J, Jang J, et al. 2006. Artificially engineered magnetic nanoparticles for ultra-sensitive molecular imaging. *Nat. Med.* 13(1):95–99
62. Yang L, Mao H, Wang YA, Cao Z, Peng X, et al. 2008. Single chain epidermal growth factor receptor antibody conjugated nanoparticles for in vivo tumor targeting and imaging. *Small* 5(2):235–43
63. Chung HJ, Castro CM, Im H, Lee H, Weissleder R. 2013. A magneto-DNA nanoparticle system for rapid detection and phenotyping of bacteria. *Nat. Nanotechnol.* 8(5):369–75

64. Perez JM, Josephson L, O'Loughlin T, Högemann D, Weissleder R. 2002. Magnetic relaxation switches capable of sensing molecular interactions. *Nat. Biotechnol.* 20(8):816–20
65. Takeda S, Mishima F, Fujimoto S, Izumi Y, Nishijima S. 2007. Development of magnetically targeted drug delivery system using superconducting magnet. *J. Magn. Magn. Mater.* 311(1):367–71
66. Rotariu O, Strachan NJC. 2005. Modelling magnetic carrier particle targeting in the tumor microvasculature for cancer treatment. *J. Magn. Magn. Mater.* 293(1):639–46
67. Feynman RP. 1970. *Feynman Lectures on Physics*. Boston: Addison Wesley Longman
68. Georgakilas V, Tzitzios V, Gournis D, Petridis D. 2005. Attachment of magnetic nanoparticles on carbon nanotubes and their soluble derivatives. *Chem. Mater.* 17(7):1613–17
69. Kim D-H, Rozhkova EA, Ulasov IV, Bader SD, Rajh T, et al. 2010. Biofunctionalized magnetic-vortex microdiscs for targeted cancer-cell destruction. *Nat. Mater.* 9(2):165–71
70. Colombo M, Carregal-Romero S, Casula MF, Gutiérrez L, Morales MP, et al. 2012. Biological applications of magnetic nanoparticles. *Chem. Soc. Rev.* 41(11):4306–34
71. Puentes VF, Krishnan KM, Alivisatos AP. 2001. Colloidal nanocrystal shape and size control: the case of cobalt. *Science* 291(5511):2115–17
72. Cozzoli PD, Snoeck E, Garcia MA, Giannini C, Guagliardi A, et al. 2006. Colloidal synthesis and characterization of tetrapod-shaped magnetic nanocrystals. *Nano Lett.* 6(9):1966–72
73. Guardia P, Pérez N, Labarta A, Batlle X. 2010. Controlled synthesis of iron oxide nanoparticles over a wide size range. *Langmuir* 26(8):5843–47
74. Wang Z, Wu L, Chen M, Zhou S. 2009. Facile synthesis of superparamagnetic fluorescent Fe₃O₄/ZnS hollow nanospheres. *J. Am. Chem. Soc.* 131(32):11276–77
75. Sun S, Zeng H, Robinson DB, Raoux S, Rice PM, et al. 2004. Monodisperse MFe₂O₄ (M = Fe, Co, Mn) nanoparticles. *J. Am. Chem. Soc.* 126(1):273–79
76. Gao J, Gu H, Xu B. 2009. Multifunctional magnetic nanoparticles: design, synthesis, and biomedical applications. *Acc. Chem. Res.* 42(8):1097–107
77. Lattuada M, Hatton TA. 2007. Preparation and controlled self-assembly of Janus magnetic nanoparticles. *J. Am. Chem. Soc.* 129(42):12878–89
78. Taboada E, Rodríguez E, Roig A, Oró J, Roch A, Muller RN. 2007. Relaxometric and magnetic characterization of ultrasmall iron oxide nanoparticles with high magnetization. Evaluation as potential T₁ magnetic resonance imaging contrast agents for molecular imaging. *Langmuir* 23(8):4583–88
79. Cheon J, Kang N-J, Lee S-M, Lee J-H, Yoon J-H, Oh SJ. 2004. Shape evolution of single-crystalline iron oxide nanocrystals. *J. Am. Chem. Soc.* 126(7):1950–51
80. Park S, Kim S, Lee S, Khim ZG, Char K, Hyeon T. 2000. Synthesis and magnetic studies of uniform iron nanorods and nanospheres. *J. Am. Chem. Soc.* 122(35):8581–82
81. Kim D, Lee N, Park M, Kim BH, An K, Hyeon T. 2009. Synthesis of uniform ferrimagnetic magnetite nanocubes. *J. Am. Chem. Soc.* 131(2):454–55
82. An K, Kwon SG, Park M, Na HB, Baik S-I, et al. 2008. Synthesis of uniform hollow oxide nanoparticles through nanoscale acid etching. *Nano Lett.* 8(12):4252–58
83. Cabot A, Puentes VF, Shevchenko E, Yin Y, Balcells L, et al. 2007. Vacancy coalescence during oxidation of iron nanoparticles. *J. Am. Chem. Soc.* 129(34):10358–60
84. Han Q, Liu Z, Xu Y, Zhang H. 2007. Synthesis and magnetic properties of single-crystalline magnetite nanowires. *J. Cryst. Growth* 307(2):483–89
85. Lübke AS, Alexiou C, Bergemann C. 2001. Clinical applications of magnetic drug targeting. *J. Surg. Res.* 95(2):200–6
86. Pankhurst QA, Connolly J, Jones SK, Dobson J. 2003. Applications of magnetic nanoparticles in biomedicine. *J. Phys. D: Appl. Phys.* 36(13):R167–81
87. Pankhurst QA, Thanh NTK, Jones SK, Dobson J. 2009. Progress in applications of magnetic nanoparticles in biomedicine. *J. Phys. D: Appl. Phys.* 42(22):224001
88. Nacev A, Komae A, Sarwar A, Probst R, Kim SH, et al. 2012. Towards control of magnetic fluids in patients: directing therapeutic nanoparticles to disease locations. *IEEE Control Syst.* 32(3):32–74
89. Polyak B, Friedman G. 2009. Magnetic targeting for site-specific drug delivery: applications and clinical potential. *Expert Opin. Drug Deliv.* 6(1):53–70

90. Bawa R. 2008. Nanoparticle-based therapeutics in humans: a survey. *Nanotech. Law Bus.* 5:135–55
91. Schuknecht HF, Merchant SN, Nadol JB Jr. 2010. *Schuknecht's Pathology of the Ear*. Shelton, CT: PMPH. 3rd ed.
92. Stachler RJ, Chandrasekhar SS, Archer SM, Rosenfeld RM, Schwartz SR, et al. 2012. Clinical practice guideline: sudden hearing loss. *Otolaryngol. Head Neck Surg.* 146(Suppl. 3):S1–35
93. Natl. Inst. Deaf. Other Commun. Disord. (NIDCD) Epidemiol. Stat. Program. 2012. *Prevalence of chronic tinnitus*. Chart, NIDCD, updated May. <http://www.nidcd.nih.gov/health/statistics/Pages/prevalence.aspx>
94. Natl. Inst. Deaf. Other Commun. Disord. 2010. *Ménière's disease*. NIH Publ. No. 10-3404, NIDCD, Bethesda, MD, updated July. <http://www.nidcd.nih.gov/health/balance/pages/meniere.aspx>
95. Salt AN, Plontke SK. 2005. Local inner-ear drug delivery and pharmacokinetics. *Drug Discov. Today* 10(19):1299–306
96. Radeloff A, Unkelbach MH, Tillein J, Braun S, Helbig S, et al. 2007. Impact of intrascalar blood on hearing. *Laryngoscope* 117(1):58–62
97. Juhn SK, Hunter BA, Odland RM. 2000. Blood-labyrinth barrier and fluid dynamics of the inner ear. *Int. Tinnitus J.* 7(2):72–83
98. Swan EEL, Mescher MJ, Sewell WF, Tao SL, Borenstein JT. 2008. Inner ear drug delivery for auditory applications. *Adv. Drug Deliv. Rev.* 60(15):1583–99
99. Li P, Zeng XL, Ye J, Yang QT, Zhang GH, Li Y. 2011. Intratympanic methylprednisolone improves hearing function in refractory sudden sensorineural hearing loss: a control study. *Audiol. Neurotol.* 16(3):198–202
100. Plaza G, Herráiz C. 2007. Intratympanic steroids for treatment of sudden hearing loss after failure of intravenous therapy. *Otolaryngol. Head Neck Surg.* 137(1):74–78
101. Haynes DS, O'Malley M, Cohen S, Watford K, Labadie RF. 2007. Intratympanic dexamethasone for sudden sensorineural hearing loss after failure of systemic therapy. *Laryngoscope* 117(1):3–15
102. Rauch SD, Halpin CF, Antonelli PJ, Babu S, Carey JP, et al. 2011. Oral versus intratympanic corticosteroid therapy for idiopathic sudden sensorineural hearing loss: a randomized trial. *JAMA* 305(20):2071–79
103. Chandrasekhar SS, Rubinstein RY, Kwartler JA, Gatz M, Connelly PE, et al. 2000. Dexamethasone pharmacokinetics in the inner ear: comparison of route of administration and use of facilitating agents. *Otolaryngol. Head Neck Surg.* 122(4):521–28
104. Sorrells SF, Sapolsky RM. 2007. An inflammatory review of glucocorticoid actions in the CNS. *Brain Behav. Immun.* 21(3):259–72
105. Sholter DE, Armstrong PW. 2000. Adverse effects of corticosteroids on the cardiovascular system. *Can. J. Cardiol.* 16(4):505–11
106. Pisu M, James N, Sampsel S, Saag KG. 2005. The cost of glucocorticoid-associated adverse events in rheumatoid arthritis. *Rheumatology (Oxford)* 44(6):781–88
107. Juhn SK. 1988. Barrier systems in the inner ear. *Acta Otolaryngol.* 105(S458):79–83
108. Labadie RF, Majdani O, Fitzpatrick JM. 2007. Image-guided technique in neurotology. *Otolaryngol. Clin. North Am.* 40(3):611–24
109. Kratchman LB, Schurzig D, McRackan TR, Balachandran R, Noble JH, et al. 2012. A manually operated, advance off-stylet insertion tool for minimally invasive cochlear implantation surgery. *IEEE Trans. Biomed. Eng.* 59(10):2792–800
110. Wang H, Northrop C, Liberman MC, Merchant SN. 2006. *3-D virtual model of a human temporal bone*. 3D Virtual Model, Eaton-Peabody Lab., Mass. Eye Ear Infirm., Boston <http://www.masseyeandear.org/research/ent/eaton-peabody/epl-imaging-resources/3-d-model-of-human-temporal-bone/>
111. Wang H, Northrop C, Burgess B, Liberman MC, Merchant SN. 2006. Three-dimensional virtual model of the human temporal bone: a stand-alone, downloadable teaching tool. *Otol. Neurotol.* 27(4):452–57
112. Hu A, Parnes LS. 2009. Intratympanic steroids for inner ear disorders: a review. *Audiol. Neurotol.* 14(6):373–82
113. Rivera T, Sanz L, Camarero G, Varela-Nieto I. 2012. Drug delivery to the inner ear: strategies and their therapeutic implications for sensorineural hearing loss. *Curr. Drug Deliv.* 9(3):231–42

114. Salt AN, Plontke SK. 2009. Principles of local drug delivery to the inner ear. *Audiol. Neurotol.* 14(6):350–60
115. Slattery WH, Fisher LM, Iqbal Z, Friedman RA, Liu N. 2005. Intratympanic steroid injection for treatment of idiopathic sudden hearing loss. *Otolaryngol. Head Neck Surg.* 133(2):251–59
116. McCall AA, Swan EEL, Borenstein JT, Sewell WF, Kujawa SG, McKenna MJ. 2010. Drug delivery for treatment of inner ear disease: current state of knowledge. *Ear Hear.* 31(2):156–65
117. Piu F, Wang X, Fernandez R, Dellamary L, Harrop A, et al. 2011. OTO-104: a sustained-release dexamethasone hydrogel for the treatment of otic disorders. *Otol. Neurotol.* 32(1):171–79
118. Salt AN, Hartsock J, Plontke S, LeBel C, Piu F. 2011. Distribution of dexamethasone and preservation of inner ear function following intratympanic delivery of a gel-based formulation. *Audiol. Neurotol.* 16(5):323–35
119. Rarey KE, Lohuis PJ, Ten Cate WJ. 1991. Response of the stria vascularis to corticosteroids. *Laryngoscope* 101(10):1081–84
120. Silverstein H. 1999. Use of a new device, the MicroWick, to deliver medication to the inner ear. *Ear Nose Throat J.* 78(8):595–98, 600
121. Suryanarayanan R, Srinivasan VR, O’Sullivan G. 2009. Transtympanic gentamicin treatment using Silverstein MicroWick in Ménière’s disease patients: long term outcome. *J. Laryngol. Otol.* 123(1):45–49
122. Weisskopf P, Hoffer ME, Kopke RD, Gottshall K, Allen K, Wester D. 2001. Microdose gentamicin delivered via the round window microcatheter: a therapeutic option in Menière’s disease. *Oper. Tech. Otolaryngol. Head Neck Surg.* 12(3):154–56
123. Plontke SK, Zimmermann R, Zenner H-P, Löwenheim H. 2006. Technical note on microcatheter implantation for local inner ear drug delivery: surgical technique and safety aspects. *Otol. Neurotol.* 27(7):912–17
124. Lee KY, Nakagawa T, Okano T, Hori R, Ono K, et al. 2007. Novel therapy for hearing loss: delivery of insulin-like growth factor 1 to the cochlea using gelatin hydrogel. *Otol. Neurotol.* 28(7):976–81
125. Paulson DP, Abuzeid W, Jiang H, Oe T, O’Malley BW, Li D. 2008. A novel controlled local drug delivery system for inner ear disease. *Laryngoscope* 118(4):706–11
126. Endo T, Nakagawa T, Kita T, Iguchi F, Kim T-S, et al. 2005. Novel strategy for treatment of inner ears using a biodegradable gel. *Laryngoscope* 115(11):2016–20
127. Kopke RD, Wassel RA, Mondalek F, Grady B, Chen K, et al. 2006. Magnetic nanoparticles: inner ear targeted molecule delivery and middle ear implant. *Audiol. Neurotol.* 11(2):123–33
128. Shellock FG. 2001. *Magnetic Resonance Procedures: Health Effects and Safety*. Boca Raton, FL: CRC. 478 pp.
129. Schenck JF. 1996. The role of magnetic susceptibility in magnetic resonance imaging: MRI magnetic compatibility of the first and second kinds. *Med. Phys.* 23(6):815–50
130. Vignaud A, Maître X, Guillot G, Durand E, de Rochefort L, et al. 2005. Magnetic susceptibility matching at the air–tissue interface in rat lung by using a superparamagnetic intravascular contrast agent: influence on transverse relaxation time of hyperpolarized helium-3. *Magn. Reson. Med.* 54(1):28–33
131. Skumryev V, Blythe HJ, Cullen J, Coey JMD. 1999. AC susceptibility of a magnetite crystal. *J. Magn. Magn. Mater.* 196:515–17
132. Heider F, Zitzelsberger A, Fabian K. 1996. Magnetic susceptibility and remanent coercive force in grown magnetite crystals from 0.1 μm to 6 mm. *Phys. Earth Planet. Inter.* 93(3–4):239–56
133. Dunlop DJ. 1984. A method of determining demagnetizing factor from multidomain hysteresis. *J. Geophys. Res.: Solid Earth* 89(B1):553–58
134. Grief AD, Richardson G. 2005. Mathematical modelling of magnetically targeted drug delivery. *J. Magn. Magn. Mater.* 293(1):455–63
135. Mikkelsen CI. 2005. *Magnetic separation and hydrodynamic interactions in microfluidic systems*. PhD Thesis, Dep. Micro Nanotechnol., Tech. Univ. Denmark, Kongens Lyngby
136. Sarwar A, Nemirovski A, Shapiro B. 2012. Optimal Halbach permanent magnet designs for maximally pulling and pushing nanoparticles. *J. Magn. Magn. Mater.* 324(5):742–54
137. Shapiro B, Dormer K, Rutel IB. 2010. A two-magnet system to push therapeutic nanoparticles. *AIP Conf. Proc.* 1311(1):77–88
138. Sarwar A, Lee R, Depireux DA, Shapiro B. 2013. Magnetic injection of nanoparticles into rat inner ears at a human head working distance. *IEEE Trans. Magn.* 49(1):440–52

139. Depireux D, Lee R, Sarwar A, Shapiro B. 2012. *Drug delivery to the inner ear of rats using magnetically steered nanoparticles*. Presented at Mid-Winter Meet. Assoc. Res. Otolaryngol., Feb. 25–29, San Diego, CA
140. Cherry DK, Woodwell DA. 2002. National ambulatory medical care survey: 2000 summary. *Adv. Data* (328):1–32
141. Rosenfeld RM, Casselbrant ML, Hannley MT. 2001. Implications of the AHRQ evidence report on acute otitis media. *Otolaryngol. Head Neck Surg.* 125(5):439–48
142. Cent. Dis. Control. Prev. (CDC). 2014. *NAMCS and NHAMCS web tables*. Ambul. Health Care Data, CDC, Atlanta, updated Feb. 24. http://www.cdc.gov/nchs/ahcd/web_tables.htm#2010
143. Rovers MM. 2008. The burden of otitis media. *Vaccine* 26(Suppl. 7):G2–4
144. Kenna MA. 2005. Otitis media and the new guidelines. *J. Otolaryngol.* 34(Suppl. 1):S24–32
145. Grubb MS, Spaugh DC. 2010. Treatment failure, recurrence, and antibiotic prescription rates for different acute otitis media treatment methods. *Clin. Pediatr.* 49(10):970–75
146. Ryan AF, Jung TTK, Juhn SK, Li J-D, Andalibi A, et al. 2005. Recent advances in otitis media. 4A. Molecular biology. *Ann. Otol. Rhinol. Laryngol. Suppl.* 194:42–49
147. Lim DJ, Birck H. 1971. Ultrastructural pathology of the middle ear mucosa in serous otitis media. *Ann. Otol. Rhinol. Laryngol.* 80(6):838–53
148. Tos M, Bak-Pedersen K. 1976. Goblet cell population in the pathological middle ear and eustachian tube of children and adults. *Ann. Otol. Rhinol. Laryngol.* 86(2 Pt. 1):209–18
149. Klein JO. 2000. The burden of otitis media. *Vaccine* 19(Suppl. 1):S2–8
150. Teele DW, Klein JO, Rosner BA. 1984. Otitis media with effusion during the first three years of life and development of speech and language. *Pediatrics* 74(2):282–87
151. Subcomm. Manag. Acute Otitis Media. 2004. Diagnosis and management of acute otitis media. *Pediatrics* 113(5):1451–65
152. Shehab N, Patel PR, Srinivasan A, Budnitz DS. 2008. Emergency department visits for antibiotic-associated adverse events. *Clin. Infect. Dis.* 47(6):735–43
153. Hoberman A, Paradise JL, Rockette HE, Shaikh N, Wald ER, et al. 2011. Treatment of acute otitis media in children under 2 years of age. *N. Engl. J. Med.* 364(2):105–15
154. Tähtinen PA, Laine MK, Huovinen P, Jalava J, Ruuskanen O, Ruohola A. 2011. A placebo-controlled trial of antimicrobial treatment for acute otitis media. *N. Engl. J. Med.* 364(2):116–26
155. Kogan MD, Overpeck MD, Hoffman HJ, Casselbrant ML. 2000. Factors associated with tympanostomy tube insertion among preschool-aged children in the United States. *Am. J. Public Health* 90(2):245–50
156. Hoskison E, Daniel M, Al-Zahid S, Shakesheff K, Bayston R, Birchall J. 2013. Drug delivery to the ear. *Ther. Deliv.* 4(1):115–24
157. Khoo X, Simons EJ, Chiang HH, Hickey JM, Sabharwal V, et al. 2013. Formulations for trans-tympanic antibiotic delivery. *Biomaterials* 34(4):1281–88
158. Campbell WR, Johnson RH, Paulsen NE. 2008. Methods for treatment and prevention of otitis media using chemical penetration enhancers to facilitate transmembrane drug delivery into the middle ear. *US Patent No. 20080269187 A1*
159. Friedman DS, O’Colmain BJ, Muñoz B, Tomany SC, McCarty C, et al. 2004. Prevalence of age-related macular degeneration in the United States. *Arch. Ophthalmol.* 122(4):564–72
160. Lee PP, Feldman ZW, Ostermann J, Brown DS, Sloan FA. 2003. Longitudinal prevalence of major eye diseases. *Arch. Ophthalmol.* 121(9):1303–10
161. Eye Dis. Preval. Res. Group. 2004. Causes and prevalence of visual impairment among adults in the United States. *Arch. Ophthalmol.* 122(4):477–85
162. Natl. Eye Inst. (NEI). 2013. *Facts about age-related macular degeneration*. Fact Sheet, NEI, Bethesda, MD, reviewed July. http://www.nei.nih.gov/health/maculardegen/armd_facts.asp#10
163. Green WR, Enger C. 2005. Age-related macular degeneration histopathologic studies: the 1992 Lorenz E. Zimmerman Lecture. *Retina* 25(5 Suppl.):1519–35
164. Michels S, Schmidt-Erfurth U, Rosenfeld PJ. 2006. Promising new treatments for neovascular age-related macular degeneration. *Expert Opin. Investig. Drugs* 15(7):779–93
165. Peyman GA, Herbst R. 1974. Bacterial endophthalmitis: treatment with intraocular injection of gentamicin and dexamethasone. *Arch. Ophthalmol.* 91(5):416–18

166. Husain D, Kramer M, Kenny AG, Michaud N, Flotte TJ, et al. 1999. Effects of photodynamic therapy using verteporfin on experimental choroidal neovascularization and normal retina and choroid up to 7 weeks after treatment. *Investig. Ophthalmol. Vis. Sci.* 40(10):2322–31
167. Dorin G. 2004. Evolution of retinal laser therapy: minimum intensity photocoagulation (MIP). Can the laser heal the retina without harming it? *Semin. Ophthalmol.* 19(1–2):62–68
168. McMeel JW, Trempe CL, Franks EB. 1977. Diabetic maculopathy. *Trans. Sect. Ophthalmol. Am. Acad. Ophthalmol. Otolaryngol.* 83(3 Pt. 1):OP476–87
169. Gillies MC, Sutter FKP, Simpson JM, Larsson J, Ali H, Zhu M. 2006. Intravitreal triamcinolone for refractory diabetic macular edema: two-year results of a double-masked, placebo-controlled, randomized clinical trial. *Ophthalmology* 113(9):1533–38
170. Berson EL. 1993. Retinitis pigmentosa: the Friedenwald Lecture. *Investig. Ophthalmol. Vis. Sci.* 34(5):1659–76
171. Hartong DT, Berson EL, Dryja TP. 2006. Retinitis pigmentosa. *Lancet* 368(9549):1795–809
172. Berson EL, Rosner B, Sandberg MA, Hayes KC, Nicholson BW, et al. 1993. A randomized trial of vitamin A and vitamin E supplementation for retinitis pigmentosa. *Arch. Ophthalmol.* 111(6):761–72
173. Sieving PA, Caruso RC, Tao W, Coleman HR, Thompson DJS, et al. 2006. Ciliary neurotrophic factor (CNTF) for human retinal degeneration: Phase I trial of CNTF delivered by encapsulated cell intraocular implants. *Proc. Natl. Acad. Sci. USA* 103(10):3896–901
174. Shantha TR, Shantha J. 2011. Retinitis pigmentosa treatment. *US Patent No. 20120101033 A1*
175. Cideciyan AV, Aleman TS, Boye SL, Schwartz SB, Kaushal S, et al. 2008. Human gene therapy for RPE65 isomerase deficiency activates the retinoid cycle of vision but with slow rod kinetics. *Proc. Natl. Acad. Sci. USA* 105(39):15112–17
176. Narfström K, Katz ML, Ford M, Redmond TM, Rakoczy E, Bragadóttir R. 2003. In vivo gene therapy in young and adult *RPE65*^{-/-} dogs produces long-term visual improvement. *J. Hered.* 94(1):31–37
177. Mello CC, Kramer JM, Stinchcomb D, Ambros V. 1991. Efficient gene transfer in *C. elegans*: extrachromosomal maintenance and integration of transforming sequences. *EMBO J.* 10(12):3959–70
178. Green M, Thorburn A, Kern R, Loewenstein PM. 2007. The use of cell microinjection for the in vivo analysis of viral transcriptional regulatory protein domains. *Methods Mol. Med.* 131:157–86
179. Williamson TH. 1997. Central retinal vein occlusion: What's the story? *Br. J. Ophthalmol.* 81(8):698–704
180. Soubrane G. 1999. Macular edema in retinal vein occlusion: up-date from the central retinal vein occlusion study. *Doc. Ophthalmol.* 97(3–4):279–82
181. Haller JA, Bandello F, Belfort R Jr, Blumenkranz MS, Gillies M, et al. 2010. Randomized, sham-controlled trial of dexamethasone intravitreal implant in patients with macular edema due to retinal vein occlusion. *Ophthalmology* 117(6):1134–46.e3
182. Haller JA, Bandello F, Belfort R Jr, Blumenkranz MS, Gillies M, et al. 2011. Dexamethasone intravitreal implant in patients with macular edema related to branch or central retinal vein occlusion: twelve-month study results. *Ophthalmology* 118(12):2453–60
183. Jonas JB, Kreissig I, Degenring RF. 2002. Intravitreal triamcinolone acetate as treatment of macular edema in central retinal vein occlusion. *Graefes Arch. Clin. Exp. Ophthalmol.* 240(9):782–83
184. Laatikainen L, Kohner EM, Khoury D, Blach RK. 1977. Panretinal photocoagulation in central retinal vein occlusion: a randomised controlled clinical study. *Br. J. Ophthalmol.* 61(12):741–53
185. Hayreh SS, Klugman MR, Podhajsky P, Servais GE, Perkins ES. 1990. Argon laser panretinal photocoagulation in ischemic central retinal vein occlusion. *Graefes Arch. Clin. Exp. Ophthalmol.* 228(4):281–96
186. Moshfeghi DM, Kaiser PK, Scott IU, Sears JE, Benz M, et al. 2003. Acute endophthalmitis following intravitreal triamcinolone acetate injection. *Am. J. Ophthalmol.* 136(5):791–96
187. Ciulla TA, Starr MB, Masket S. 2002. Bacterial endophthalmitis prophylaxis for cataract surgery: an evidence-based update. *Ophthalmology* 109(1):13–24
188. Taban M, Behrens A, Newcomb RL, Nobe MY, Saedi G, et al. 2005. Acute endophthalmitis following cataract surgery: a systematic review of the literature. *Arch. Ophthalmol.* 123(5):613–20
189. West ES, Behrens A, McDonnell PJ, Tielsch JM, Schein OD. 2005. The incidence of endophthalmitis after cataract surgery among the U.S. Medicare population increased between 1994 and 2001. *Ophthalmology* 112(8):1388–94

190. Olson JC, Flynn HW Jr, Forster RK, Culbertson WW. 1983. Results in the treatment of postoperative endophthalmitis. *Ophthalmology* 90(6):692–99
191. Winward KE, Pflugfelder SC, Flynn HW Jr, Roussel TJ, Davis JL. 1993. Postoperative *Propionibacterium* endophthalmitis: treatment strategies and long-term results. *Ophthalmology* 100(4):447–51
192. Gaudana R, Ananthula HK, Parenky A, Mitra AK. 2010. Ocular drug delivery. *AAPS J.* 12(3):348–60
193. Barar J, Javadzadeh AR, Omid Y. 2008. Ocular novel drug delivery: impacts of membranes and barriers. *Expert Opin. Drug Deliv.* 5(5):567–81
194. Xu Q, Kambhampati SP, Kannan RM. 2013. Nanotechnology approaches for ocular drug delivery. *Middle East Afr. J. Ophthalmol.* 20(1):26–37
195. Edelhauser HF, Rowe-Rendleman CL, Robinson MR, Dawson DG, Chader GJ, et al. 2010. Ophthalmic drug delivery systems for the treatment of retinal diseases: basic research to clinical applications. *Investig. Ophthalmol. Vis. Sci.* 51(11):5403–20
196. Al-Saikhani FI. 2013. The gene therapy revolution in ophthalmology. *Saudi J. Ophthalmol.* 27(2):107–11
197. Jager RD, Aiello LP, Patel SC, Cunningham ET. 2004. Risks of intravitreal injection: a comprehensive review. *Retina* 24(5):676–98
198. Kalam MA, Sultana Y, Samad A, Ali A, Aqil M, et al. 2008. Gelrite-based in vitro gelation ophthalmic drug delivery system of gatifloxacin. *J. Dispers. Sci. Technol.* 29(1):89–96
199. Alonso MJ, Sánchez A. 2003. The potential of chitosan in ocular drug delivery. *J. Pharm. Pharmacol.* 55(11):1451–63
200. Callanan D, Williams P. 2008. Topical nepafenac in the treatment of diabetic macular edema. *Clin. Ophthalmol.* 2(4):689–92
201. Weiner AL, Gilger BC. 2010. Advancements in ocular drug delivery. *Vet. Ophthalmol.* 13(6):395–406
202. Prow T, Grebe R, Merges C, Smith JN, McLeod DS, et al. 2006. Nanoparticle tethered antioxidant response element as a biosensor for oxygen induced toxicity in retinal endothelial cells. *Mol. Vis.* 12:616–25
203. Prow TW, Bhutto I, Kim SY, Grebe R, Merges C, et al. 2008. Ocular nanoparticle toxicity and transfection of the retina and retinal pigment epithelium. *Nanomed.: Nanotechnol. Biol. Med.* 4(4):340–49
204. Dengler M, Saatchi K, Dailey JP, Matsubara J, Mikelberg FS, et al. 2010. Targeted delivery of magnetic cobalt nanoparticles to the eye following systemic administration. *AIP Conf. Proc.* 1311(1):329–36
205. Raju HB, Hu Y, Vedula A, Dubovy SR, Goldberg JL. 2011. Evaluation of magnetic micro- and nanoparticle toxicity to ocular tissues. *PLoS ONE* 6(5):e17452
206. Winkler BS, Boulton ME, Gottsch JD, Sternberg P. 1999. Oxidative damage and age-related macular degeneration. *Mol. Vis.* 5:32
207. Beatty S, Koh H-H, Phil M, Henson D, Boulton M. 2000. The role of oxidative stress in the pathogenesis of age-related macular degeneration. *Surv. Ophthalmol.* 45(2):115–34
208. Humayun MS, Prince M, de Juan E Jr, Barron Y, Moskowitz M, et al. 1999. Morphometric analysis of the extramacular retina from postmortem eyes with retinitis pigmentosa. *Investig. Ophthalmol. Vis. Sci.* 40(1):143–48
209. Shen Z, Nacev A, Sarwar A, Lee R, Depireux D, Shapiro B. 2013. Automated fluorescence and reflectance coregistered 3-D tissue imaging system. *IEEE Trans. Magn.* 49(1):279–84
210. Shen Z, Nacev A, Shapiro B. 2012. *Fluorescence and reflectance co-registered 3D tissue imaging system based on a cryostat*. Presented at Int. Conf. Sci. Clin. Appl. Magn. Carriers, 9th, Minneapolis, MN
211. Kummer MP, Abbott JJ, Kratochvil BE, Borer R, Sengul A, Nelson BJ. 2010. OctoMag: an electromagnetic system for 5-DOF wireless micromanipulation. *IEEE Trans. Robot.* 26(6):1006–17
212. Ergeneman O, Chatzipirpiridis G, Pokki J, Marin-Suárez M, Sotiriou GA, et al. 2012. In vitro oxygen sensing using intraocular microrobots. *IEEE Trans. Biomed. Eng.* 59(11):3104–9
213. Ullrich F, Bergeles C, Pokki J, Ergeneman O, Erni S, et al. 2013. Mobility experiments with microrobots for minimally invasive intraocular surgery. *Investig. Ophthalmol. Vis. Sci.* 54(4):2853–63
214. Bergeles C, Kummer MP, Kratochvil BE, Framme C, Nelson BJ. 2011. Steerable intravitreal inserts for drug delivery: in vitro and ex vivo mobility experiments. In *Medical Image Computing and Computer-Assisted Intervention—MICCAI 2011*, ed. G Fichtinger, A Martel, T Peters, pp. 33–40. Berlin: Springer

215. Gupta PK, Jensen PS Jr, de Juan E Jr. 1999. Surgical forces and tactile perception during retinal microsurgery. In *Medical Image Computing and Computer-Assisted Intervention—MICCAI 1999*, ed. C Taylor, A Colchester, pp. 1218–25. Berlin: Springer
216. Singhy SPN, Riviere CN. 2002. Physiological tremor amplitude during retinal microsurgery. *Proc. IEEE 28th Annu. Northeast Bioeng. Conf., Philadelphia*, pp. 171–72. New York: IEEE
217. Jagtap AD, Riviere CN. 2004. Applied force during vitreoretinal microsurgery with handheld instruments. *Proc. 26th Annu. Int. Conf. IEEE Eng. Med. Biol. Soc. (IEMBS '04)*, 1:2771–73. New York: IEEE
218. Mathieu JB, Martel S. 2009. IMP-aggregation of magnetic microparticles in the context of targeted therapies actuated by a magnetic resonance imaging system. *J. Appl. Phys.* 106(4):044904
219. Evans BA, Shields AR, Carroll RL, Washburn S, Falvo MR, Superfine R. 2007. Magnetically actuated nanorod arrays as biomimetic cilia. *Nano Lett.* 7(5):1428–34
220. Cordente N, Respaud M, Senocq F, Casanove M-J, Amiens C, Chaudret B. 2001. Synthesis and magnetic properties of nickel nanorods. *Nano Lett.* 1(10):565–68
221. Nacev A, Beni C, Bruno O, Shapiro B. 2011. The behaviors of ferro-magnetic nano-particles in and around blood vessels under applied magnetic fields. *J. Magn. Magn. Mater.* 323(6):651–68
222. Nacev A, Beni C, Bruno O, Shapiro B. 2010. Magnetic nanoparticle transport within flowing blood and into surrounding tissue. *Nanomedicine* 5(9):1459–66
223. Nacev A, Kim SH, Rodriguez-Canales J, Tangrea MA, Shapiro B, Emmert-Buck MR. 2011. A dynamic magnetic shift method to increase nanoparticle concentration in cancer metastases: a feasibility study using simulations on autopsy specimens. *Int. J. Nanomed.* 6(1):2907–23
224. Renkin EM. 1954. Filtration, diffusion, and molecular sieving through porous cellulose membranes. *J. Gen. Physiol.* 38(2):225–43
225. Ogston AG, Preston BN, Wells JD. 1973. On the transport of compact particles through solutions of chain-polymers. *Proc. R. Soc. Lond. A Math. Phys. Sci.* 333(1594):297–316
226. Kulkarni S, Nacev A, Ramaswamy B, Depireux D, Shapiro B. 2013. *Understanding motion of magnetic nanoparticles in tissue*. Presented at Front. Biomagn. Nanopart. III, June 2–5, Telluride, CO
227. Salt AN, Ohyama K, Thalmann R. 1991. Radial communication between the perilymphatic scalae of the cochlea. II: Estimation by bolus injection of tracer into the sealed cochlea. *Hear. Res.* 56(1–2):37–43
228. Hiemenz PC, Rajagopalan R. 1997. *Principles of Colloid and Surface Chemistry*. Boca Raton, FL: CRC. 676 pp. 3rd ed.
229. Saltzman WM. 2001. *Drug Delivery: Engineering Principles for Drug Therapy*. New York: Oxford Univ. Press
230. Fournier RL. 2007. *Basic Transport Phenomena in Biomedical Engineering*. New York: Taylor & Francis
231. Lai SK, O'Hanlon DE, Harrold S, Man ST, Wang Y-Y, et al. 2007. Rapid transport of large polymeric nanoparticles in fresh undiluted human mucus. *Proc. Natl. Acad. Sci. USA* 104(5):1482–87
232. Lai SK, Wang Y-Y, Hanes J. 2009. Mucus-penetrating nanoparticles for drug and gene delivery to mucosal tissues. *Adv. Drug Deliv. Rev.* 61(2):158–71
233. Sun C, Lee J, Zhang M. 2008. Magnetic nanoparticles in MR imaging and drug delivery. *Adv. Drug Deliv. Rev.* 60(11):1252–65
234. Weizenecker J, Gleich B, Rahmer J, Dahnke H, Borgert J. 2009. Three-dimensional real-time in vivo magnetic particle imaging. *Phys. Med. Biol.* 54(5):L1–10
235. Kim BH, Lee N, Kim H, An K, Park YI, et al. 2011. Large-scale synthesis of uniform and extremely small-sized iron oxide nanoparticles for high-resolution T_1 magnetic resonance imaging contrast agents. *J. Am. Chem. Soc.* 133(32):12624–31
236. Weinberg IN, Stepanov PY, Fricke ST, Probst R, Urdaneta M, et al. 2012. Increasing the oscillation frequency of strong magnetic fields above 101 kHz significantly raises peripheral nerve excitation thresholds. *Med. Phys.* 39(5):2578–83
237. Gleich B, Weizenecker J. 2005. Tomographic imaging using the nonlinear response of magnetic particles. *Nature* 435(7046):1214–17
238. Rahmer J, Antonelli A, Sfara C, Tiemann B, Gleich B, et al. 2013. Nanoparticle encapsulation in red blood cells enables blood-pool magnetic particle imaging hours after injection. *Phys. Med. Biol.* 58(12):3965–77



Contents

Heart Regeneration with Engineered Myocardial Tissue <i>Kareem L.K. Coulombe, Vivek K. Bajpai, Stelios T. Andreadis, and Charles E. Murry</i> ...	1
Bioengineering the Ovarian Follicle Microenvironment <i>Lonnie D. Shea, Teresa K. Woodruff, and Ariella Shikanov</i>	29
Computational Modeling of Cardiac Valve Function and Intervention <i>Wei Sun, Caitlin Martin, and Thuy Pham</i>	53
Blood Substitutes <i>Andre F. Palmer and Marcos Intaglietta</i>	77
Optical Neural Interfaces <i>Melissa R. Warden, Jessica A. Cardin, and Karl Deisseroth</i>	103
From Unseen to Seen: Tackling the Global Burden of Uncorrected Refractive Errors <i>Nicholas J. Durr, Shivang R. Dave, Eduardo Lage, Susana Marcos, Frank Thorn, and Daryl Lim</i>	131
Photoacoustic Microscopy and Computed Tomography: From Bench to Bedside <i>Libong V. Wang and Liang Gao</i>	155
Effects of Biomechanical Properties of the Bone–Implant Interface on Dental Implant Stability: From In Silico Approaches to the Patient’s Mouth <i>Guillaume Haïat, Hom-Lay Wang, and John Brunski</i>	187
Sound-Producing Voice Prostheses: 150 Years of Research <i>G.J. Verkerke and S.L. Thomson</i>	215
3D Biofabrication Strategies for Tissue Engineering and Regenerative Medicine <i>Piyush Bajaj, Ryan M. Schweller, Ali Khadembosseini, Jennifer L. West, and Rashid Bashir</i>	247
Induced Pluripotent Stem Cells for Regenerative Medicine <i>Karen K. Hirschi, Song Li, and Krishnendu Roy</i>	277

Electroporation-Based Technologies for Medicine: Principles, Applications, and Challenges <i>Martin L. Yarmush, Alexander Golberg, Gregor Serša, Tadej Kotnik, and Damijan Miklavčič</i>	295
The Role of Mechanical Forces in Tumor Growth and Therapy <i>Rakesh K. Jain, John D. Martin, and Triantafyllos Stylianopoulos</i>	321
Recent Advances in Nanoparticle-Mediated siRNA Delivery <i>John-Michael Williford, Juan Wu, Yong Ren, Maani M. Archang, Kam W. Leong, and Hai-Quan Mao</i>	347
Inertial Focusing in Microfluidics <i>Joseph M. Martel and Mehmet Toner</i>	371
Electrical Stimuli in the Central Nervous System Microenvironment <i>Deanna M. Thompson, Abigail N. Koppes, John G. Hardy, and Christine E. Schmidt</i>	397
Advances in Computed Tomography Imaging Technology <i>Daniel Thomas Ginat and Rajiv Gupta</i>	431
Shaping Magnetic Fields to Direct Therapy to Ears and Eyes <i>B. Shapiro, S. Kulkarni, A. Nacev, A. Sarwar, D. Preciado, and D.A. Depireux</i>	455
Electrical Control of Epilepsy <i>David J. Mogul and Wim van Drongelen</i>	483
Mechanosensing at the Vascular Interface <i>John M. Tarbell, Scott I. Simon, and Fitz-Roy E. Curry</i>	505

Indexes

Cumulative Index of Contributing Authors, Volumes 7–16	533
Cumulative Index of Article Titles, Volumes 7–16	537

Errata

An online log of corrections to *Annual Review of Biomedical Engineering* articles may be found at <http://bioeng.annualreviews.org/>